Master's thesis

NTNU
Norwegian University of Science and Technology
Faculty of Information Technology and Electrical Engineering
Department of Engineering Cybernetics

Ola Johan Olimb Kirkerud

COLREGs-Aware Collision Avoidance for Autonomous Surface Vehicles using Encounter-Specific Artificial Potential Fields

Master's thesis in Cybernetics and Robotics
Supervisor: Morten Breivik
Co-supervisor: Emil Hjelseth Thyri
June 2022

NTNU
Norwegian University of
Science and Technology

Ola Johan Olimb Kirkerud

COLREGs-Aware Collision Avoidance for Autonomous Surface Vehicles using Encounter-Specific Artificial Potential Fields

Master's thesis in Cybernetics and Robotics
Supervisor: Morten Breivik
Co-supervisor: Emil Hjelseth Thyri
June 2022

Norwegian University of Science and Technology
Faculty of Information Technology and Electrical Engineering
Department of Engineering Cybernetics

NTNU
Norwegian University of
Science and Technology

Summary

There are many different levels of autonomy, where full autonomy is the absolute most demanding level to produce. Full autonomy requires a system that is independent of human interaction. To achieve this for an autonomous surface vehicle (ASV), it must be able to understand its surroundings, and make a plan on how it will navigate to reach its goal safely. The system responsible for ensuring safe navigation, is often referred to as a collision avoidance (COLAV) system.

In this Master's thesis, a COLAV method for ASVs is proposed. The method works as a reactive layer in the COLAV system. It uses information about the environment and its nominal trajectory, to determine position and velocity references that ensures collision free and Convention on the International Regulations for Preventing Collisions at Sea (COLREGs)-aware navigation. The nominal trajectory is constructed such that it is collision free to any static obstacles. The proposed method continuously monitors the estimated time to the closest point of approach (CPA) and the distance at the CPA between itself and other vessels to detect potential collisions. A classifier is then used to classify the encounter geometry with respect to the COLREGs rules. The method handles all vessel-to-vessel (V2V) encounters independently, by creating a unique target ship domain for each target ship (TS), where the domain is specific to the rule that applies. The targetship domain is then used in an artificial potential field (APF) to calculate reference signals for the own ship (OS) dynamic positioning system.

A simulator is developed to verify the performance of the method. The vessel and thruster model parameters are determined from the parameters used in the prototype autonomous passenger ferry milliAmpere simulator. The simulator is capable of simulating multiple ships with different behaviours.

The performance of the method is demonstrated through a large set of V2V encounters, where it handles every encounter in accordance to the COLREGs rules 13-15 and 17. The performance of the method is further demonstrated on more complex multi-vessel encounters, and through the introduction of static obstacles in the simulation environment. The method is finally compared to an APF-based COLREGs-unaware COLAV method.

Sammendrag

Det er mange ulike nivåer av autonomi, hvor full autonomi er det absolutt mest krevende nivået å produsere. Full autonomi krever et system som er uavhengig av menneskelig interaksjon. For å oppnå dette for et autonomt overflatefartøy (ASV), må systemet forstå omgivelsene, og lage en plan for hvordan den skal navigere for å nå målet sitt trygt. Systemet som er ansvarlig for å lage planene som sikrer trygg navigering, er ofte referert til som et kollisjonsungåelses-system (COLAV-system).

I denne masteroppgaven foreslås en COLAV-metode for autonome passasjerferger. Metoden fungerer som et reaktivt lag i COLAV-systemet. Den bruker informasjon om miljøet og dets nominelle bane, for å bestemme posisjons- og hastighetsreferanser som sikrer kollisjonsfri og Konvensjon om Internasjonale Regler til Forebygging av Sammenstøt på Sjøen (COLREGs)-kompatibel navigering. Den nominelle banen er konstruert slik at den er kollisjonsfri for statiske hindringer. Den foreslåtte metoden overvåker kontinuerlig den estimerte tiden til det nærmeste tilnærmingspunktet (CPA) og avstanden ved CPA mellom seg selv og andre fartøyer, for å oppdage potensielle kollisjoner. En klassifiserings metode brukes deretter for å klassifisere møtegeometrien med respekt til COLREGs reglene. Metoden håndterer alle fartøy-til-fartøy (V2V) møter individuelt, ved å lage et unikt målskip domene for hvert hinderfartøy, der domenet er spesifikt til regelen som gjelder. Målskipets domene brukes deretter i et kunstig potensial felt (APF) for å beregne referansesignaler for fartøyets dynamiske posisjoneringssystem.

En simulator er blitt utviklet for å verifisere ytelsen til metoden. Fartøy og thruster modell parametere ble bestemt fra parameterne som blir brukt i prototyp autonome passasjerfergen milliAmpere, sin simulator. Simulatoren er i stand til å simulere flere skip med ulik oppførsel.

Ytelsen til metoden demonstreres gjennom et stort sett med V2V-møter, hvor den håndterer hvert møte i samsvar med COLREGs reglene 13-15 og 17. Ytelsen til metoden demonstreres videre på mer komplekse møter med flere fartøyer, og gjennom introduksjonen av statiske hindringer i simuleringsmiljøet. Metoden sammenlignes til slutt med en APF-basert COLREGs uvitende COLAV-metode.

Preface

With this Master thesis I finalize my degree in Cybernetics and Robotics at the Norwegian University of Science and Technology (NTNU) in Trondheim. During my time in Trondheim I've had the privilege of expanding my theoretical and practical understanding of developing autonomous systems from leading researchers. Writing this thesis has been demanding, but also very rewarding. Creating a collision avoidance system is something I did not have much experience with, but the challenge has proved to be enjoyable and inspiring.

I would like to express my most sincere gratitude to my supervisors Morten Breivik and Emil Thyri, for the time they have dedicated to guide and assist me during the past 2 semesters. I would also like to thank the student organizations Revolve NTNU and Ascend NTNU for giving me the platform to embed my theoretical knowledge into practice.

- During the semester, my supervisors have assisted me during bi-weekly meetings, where the progress of the thesis and related topics have been discussed.
- A simulator was implemented in python to facilitate the testing. The vessel and thruster model parameters were borrowed from the official milliAmpere simulator.

Ola Kirkerud
Trondheim, 12 June 2022

Table of Contents

List of Tables

List of Figures

Abbreviations

ASVs = Autonomous surface vehicles
COLAV = Collision avoidance
CPA = Closest point of approach
COLREGs = Convention on the International Regulations for Preventing Collisions at Sea
APF = Artificial potential field
ENC = Electronic nautical charts
DNSD = Dynamic navigation ship domain
OS = Own-ship
TS = Target-ship
V2V = Vessel-to-vesselm
NED = North, East, Down
CPA = Closest point of approach

Chapter 1

Introduction

In this chapter, an introduction to this master thesis is given. First, the motivation behind the work is presented, then relevant previous work on this topic and a detailed description of this thesis and the author's contribution to the problem are presented. Lastly, an outline of the report is given.

1.1 Motivation

As the new industrial revolution (Industry 4.0) is evolving, it will through determined development and deployment of autonomous systems, revolutionize the way we look at transportation. The revolution is already well underway in the automotive industry, where the road is full of vehicles which operates at a partial level of autonomy, such as Tesla cars running the Tesla Autopilot[1]. Vehicles with a high level of autonomy are also being tested and deployed in the real world. An article in Press reported about the American autonomous taxi company *Cruise AV*, has gotten the green light from the Californian government to start transporting charging costumers in San Francisco. And the electric autonomous container vessel *Zhi Fei* was earlier this year put into commercial service after an extensive trial period, becoming the worlds first autonomous electric container vessel, written in Executive. There is also a focus on developing smaller autonomous surface vessels, such as ferries. Zeabuz[2] is a spin-off from the leading research community on autonomous vessels at NTNU in Trondheim and focus on developing electric autonomous passenger ferries. Having produced the prototype vessels milliAmpere and milliAmpere 2, the company has gotten a lot of attention in the media. Where an article in NRK reported that a french delegation recently visited the company, as they consider using their vessels under the 33. Olympic summer games in Paris NRK.

---

[1] `https://www.tesla.com/autopilot`

[2] `https://www.zeabuz.com/`

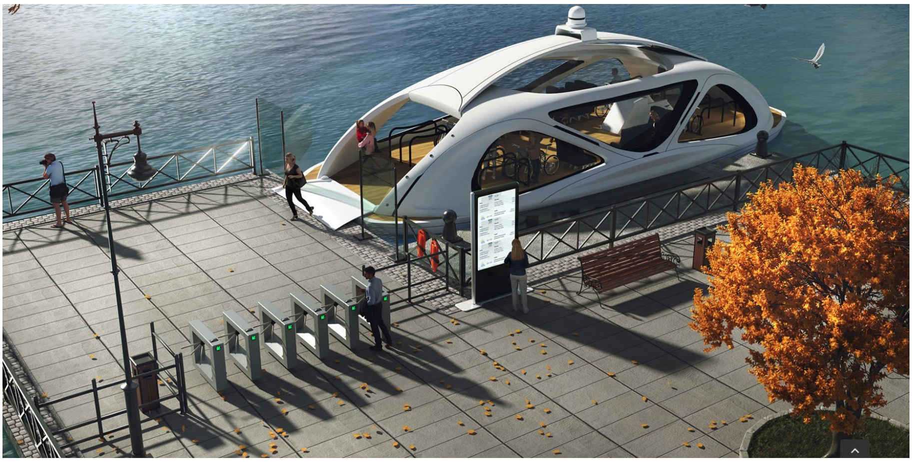

Figure 1.1: Autonomous electrical passenger ferry concept. Courtesy of Zeabuz.

A dramatic urbanization require an innovative approach when evaluating the future infrastructure of the transportation sector. When expanding on existing infrastructure on land it is usually very costly and require a lot of real estate. Real estate that could be used to build homes for the growing population. Utilizing the waterways through electric autonomous ferries, could be a climate friendly, low cost transportation alternative that have a low environmental impact on the area.

Research on the topic of the autonomous systems for surface vessels, are however far from complete. For a vessel to be fully autonomous the system must sense, perceive, plan and act without intervention. First, it must sense important information in its environment. Then, it must actually understand what it is sensing, by interpreting the raw sensor data into useful information about its environment. Then, based on the information about its environment, it must make a plan. Lastly, it must carry out the actions that the plan calls out for.

In this project, the focus will be on the perceive, plan and act part of the autonomous pipeline, specifically for a collision avoidance (COLAV) system. An example of a three layered-hybrid COLAV system architecture is presented in Figure 1.2. First, the system try to understand the environment it is in. This is done by predicting the trajectories of obstacles and using electronic nautical charts (ENC) to asses the risk of collision and interpreting the situation into the Convention on the International Regulations for Preventing Collisions at Sea (COLREGs) rules. The system then must make a plan based on the information about the environment. A three layered-hybrid COLAV system architecture is used to split the problem into different parts. First, typically even before the vessel has started its operation, it creates a nominal trajectory that navigates safely from A to B, avoiding any static obstacles. If an encounter is considered to have a risk of collision, that is not immediate, the Mid-level COLAV is typically triggered, producing a modified optimized trajectory. If an encounter has a risk of a collision that is immediate, the Short-term COLAV is triggered. This is a reactive layer, ensuring the baseline safety of the hybrid

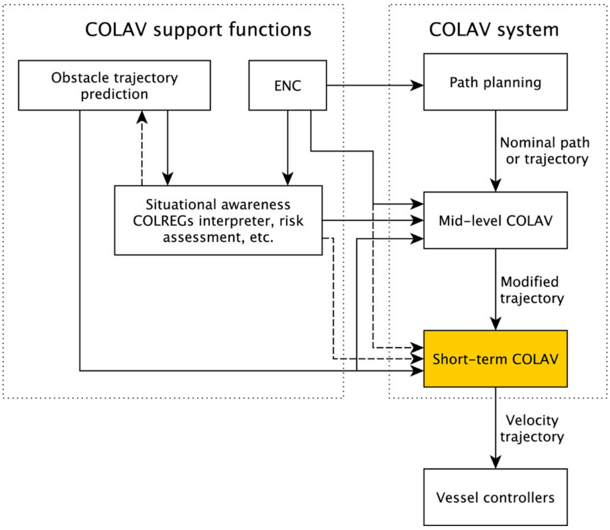

Figure 1.2: Proposition of a three layered-hybrid COLAV system architecture. Courtesy of Eriksen and Breivik (2017).

system. Lastly the Vessel controllers act out the actions to perform the COLAV systems plan. The proposed COLREGs-aware COLAV method in this theses is a reactive method, and is therefor naturally placed in the short-term COLAV layer.

1.2 Previous work

Artificial potential fields was first introduced in Khatib (1985). The paper introduced a unique real-time obstacle avoidance approach, at a time where robot collision avoidance had been a component of higher levels of control in hierarchical robot control system. In the APF approach the manipulator navigates in a field of forces. The goal position is an attractive pole for the end-effector, and the obstacles are repulsive surfaces for the manipulator parts. The most promising direction for the manipulator is found as the negative gradient of the sum of the attractive forces and the repulsive forces. Since the optimization is done by gradient decent, there is a possibility for the manipulator to get stuck in a local minima. This can occur if the manipulator has navigated into a non-convex shaped obstacles, as visualized in Figure 1.3. The are many proposed solutions to the local minima problem. In Fu-guang et al. (2005) the author's presents a virtual potential field, that pushes the manipulator towards an open space, while in Matoui et al. (2015) the author's presents a method to solve the local minima problem by couple the potential field method in a stochastic method. In an event where the manipulator has reached a local minimum, the stochastic method is then used to navigate the manipulator out of it. Monte Carlo simulated annealing or an ant colony algorithm may be used as the stochastic method.

In Huang et al. (2020) the authors presents a ship-to-ship avoidance method by implementing the cooperative ship domain model with the APF method. The method proposed

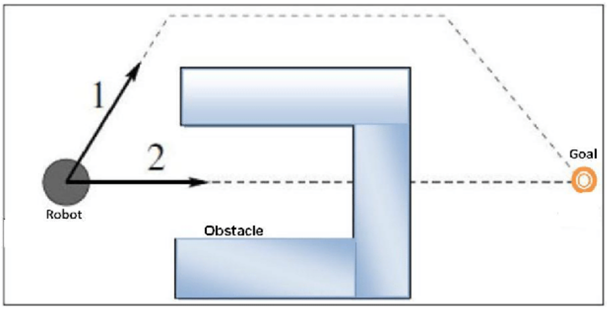

Figure 1.3: Potential field local minimum. Courtesy of Matoui et al. (2015).

is tested in two crossing situations. In the first a vessel gives way to another vessel, and in the second the give-way vessel fails to take collision avoidance measures, and the stand-on vessel must make an evasive maneuver. The cooperative ship domain model is a symmetrical circle, with center at the vessel center, and a radius dependent on both vessels length. The authors conclude that the method is fully compliant with COLREGs, which is correct for the simulations that is provided in the paper. The simulations are however quite limited, and do not provide evidence for the robustness of the method.

In Deng et al. (2021), the authors present a dynamic navigation ship domain (DNSD)-based dynamic obstacle avoidance approach for USVs with the velocity obstacle method in compliance with COLREGs. The DNSD is composed of a semi-ellipse and a semi-circle, dependent on the ship dimensions, the relative speed, the maneuverability and the encounter situation regarding the relative bearing and COLREGs. In the paper simulations with different scenarios are presented, both in single vessel-to-vessel (V2V) encounters and in multi-vessel encounters. The method proves to work nicely, however when the vessel must navigate through multiple other vessels it looks at each vessel independently. This could prove to be sub-optimal in some situations.

1.3 Problem description

In this master thesis, a reactive collision avoidance method is proposed on a vessel tracking a predefined trajectory in a known environment. The vessel is navigating in an environment with other vessels present. Situations are designed such that collisions are guaranteed if the vessels follow the predefined the trajectories. Static object are also placed in the environment, representing shallow waters or land.

The following objectives are proposed for this project:

- Develop a simulator in python with a complete vessel model and COLREGs classifier.
- Develop an APF-based COLREGs-aware reactive COLAV method.
- Verify the performance of the COLAV method through numerical simulations.

- Compare the performance of the COLAV method with a minimum standard APF.

1.4 Contributions

The contributions of this Master's thesis are

- A simulator developed in python, implemented with situational awareness module that calculates the risk of collision and a COLREGs classification. The simulator use the model parameters for the milliAmpere autonomous prototype vessel, determined in Pedersen (2019).
- A COLREGs-aware APF-based reactive COLAV method is developed to perform COLREGs compliant navigation when performing evasive maneuvers. The method is verified through numerical simulations, providing evidence for the robustness of the method.
- The COLAV method is benchmarked against a minimum standard APF.

1.5 Outline

Chapter 2 gives some theoretical background, in Chapter 3 a detailed description of the proposed COLAV method is presented, in Chapter 4 simulation results are presented and discussed, while in Chapter 5 the conclusion and future work are presented.

Chapter 2

Theoretical background

In this chapter, some of the fundamental theoretical background for this master thesis is presented, as well as some core concepts and terms.

2.1 Vessel model

2.1.1 Kinematics

NED

The North-East-Down (NED) coordinate system, denoted hereby as $\{n\}$, is a used to describe the position and orientation of the vessel. Here the x-axis points towards north, the y-axis towards east and the z-axis points down, normal to the surface of the earth. $\{n\}$ is usually a noninertial reference frame, however if the navigational area is sufficiently small, the area can be assumed flat earthed and $\{n\}$ an inertial frame, implying that the Newton's laws still apply.

In this project we assume flat earth navigation of surface vessels, meaning that the z-axis can be neglected. Giving the position and orientation of a vessel in the $\{n\}$ frame denoted as $\boldsymbol{\eta} = [X, Y, \psi]^T$, where the ψ is the orientation of the vessel. The velocity in $\{n\}$ is denoted $\dot{\boldsymbol{\eta}} = [\dot{X}, \dot{Y}, r]^T$, where $\dot{X}$ is the velocity in the North direction, $\dot{Y}$ is the velocity in the East direction and r is the rotational velocity of the vessel around the Z-axis.

Body

The noninertial body coordinate system denoted $\{b\}$ is a coordinate frame fixed to the origin and center of rotation (COR) of a vessel. The $\{b\}$ frame is used to define the linear and rotational velocity of a vessel. The x-axis is linear aligned with the longitudinal axis of the vessel, the y-axis points straight starboard and the Z-axis downwards completing the

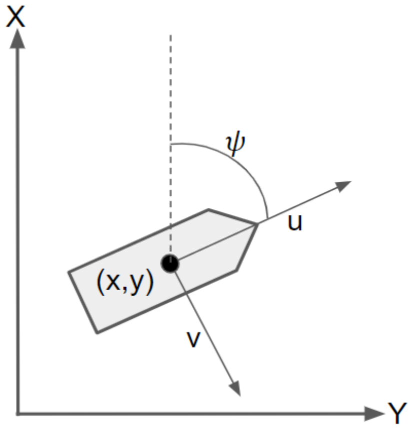

Figure 2.1: 3-DOF vessel described by position in NED frame where X is North and Y is East, the velocity is represented in the body frame and rotation in yaw.

left-hand system. This gives $\boldsymbol{\nu} = [u, v, r]^T$, where u is the velocity along the Z-axis, v the velocity aligned with the Y-axis, and r is the rotational velocity around the Z-axis.

As flat earth is assumed in this project, a combination of the $\{n\}$ frame and the $\{b\}$ frame is used to describe the entire system with 3 degrees of freedom (DOF). A visualization of this can be seen in Figure 2.1. The rotation from $\{b\}$ to $\{n\}$ is a rotation around the Z-axis, as the Z-axis is parallel for both the $\{b\}$ and $\{n\}$. This gives the rotation matrix:

$$\boldsymbol{J}_\theta(\eta) = R_{z,\psi} = \begin{bmatrix} cos(\psi) & -sin(\psi) & 0 \\ sin(\psi) & cos(\psi) & 0 \\ 0 & 0 & 1 \end{bmatrix} \tag{2.1}$$

$$\tag{2.2}$$

The relationship between the NED and body velocities can then be described as

$$\dot{\boldsymbol{\eta}} = \boldsymbol{R}(\psi)\boldsymbol{\nu} \tag{2.3}$$

where $\boldsymbol{R}(\psi) := \boldsymbol{R}_{z,\psi}$.

2.1.2 Kinetics

To develop a simulation environment, a kinetic model of the vessel must be implemented. A 3 DOF model in the horizontal plane introduced in Fossen (2000) is presented in this subsection. The manoeuvring model is based on the rigid-body kinetics

$$\boldsymbol{M}_{RB}\dot{\boldsymbol{\nu}} + \boldsymbol{C}_{RB}(\boldsymbol{\nu})\boldsymbol{\nu} = \tau_{RB} \tag{2.4}$$

$$\boldsymbol{\tau}_{RB} = \boldsymbol{\tau}_{hyd} + \boldsymbol{\tau}_{hs} + \boldsymbol{\tau}_{wind} + \boldsymbol{\tau}_{wave} + \boldsymbol{\tau}. \tag{2.5}$$

Here, $\boldsymbol{\tau}$ represents the forces of the actuators on the vessel, while $\boldsymbol{\tau}_{wind}$ and $\boldsymbol{\tau}_{wave}$ are respectively wind and wave forces. $\boldsymbol{\tau}_{hs} = 0$ as the model only works in the horizontal plane. The hydrodynamic forces can be calculated as:

$$\boldsymbol{\tau}_{hyd} = -\boldsymbol{M}_{A}\dot{\boldsymbol{\nu}}_r - \boldsymbol{C}_{A}(\boldsymbol{\nu}_r)\boldsymbol{\nu}_r - \boldsymbol{D}(\boldsymbol{\nu}_r)\boldsymbol{\nu}_r \tag{2.6}$$

where $\boldsymbol{M}_A$ is the added mass matrix, $\boldsymbol{C}_A$ the Coriolis and centripetal matrix and $\boldsymbol{D}$ the viscous and wave induced damping matrix. By combining (2.4-2.6) we get:

$$\boldsymbol{M}_{RB}\dot{\boldsymbol{\nu}} + \boldsymbol{M}_{A}\dot{\boldsymbol{\nu}} + \boldsymbol{C}_{A}(\boldsymbol{\nu}_r)\boldsymbol{\nu}_r\boldsymbol{D}(\boldsymbol{\nu}_r)\boldsymbol{\nu} = \boldsymbol{\tau}_{wind} + \boldsymbol{\tau}_{wave} + \boldsymbol{\tau}. \tag{2.7}$$

Ocean currents causes $\boldsymbol{\nu_r}$ not equal to $\boldsymbol{\nu}$. By assuming constant current and parameterizing $\boldsymbol{C}_{RB}$ independent of the linear velocity, the system can then be written on the form

$$\boldsymbol{M}\dot{\boldsymbol{\nu}}_r + \boldsymbol{C}(\boldsymbol{\nu}_r)\boldsymbol{\nu}_r + \boldsymbol{D}(\boldsymbol{\nu}_r)\boldsymbol{\nu}_r = \boldsymbol{\tau}_{wind} + \boldsymbol{\tau}_{wave} + \boldsymbol{\tau}, \tag{2.8}$$

$$\boldsymbol{M} = \boldsymbol{M}_{RB} + \boldsymbol{M}_{A}, \tag{2.9}$$

$$\boldsymbol{C}(\boldsymbol{\nu}_r) = \boldsymbol{C}_{RB}(\boldsymbol{\nu}) + \boldsymbol{C}_{A}(\boldsymbol{\nu}_r). \tag{2.10}$$

2.2 Artificial potential field

The APF is constructed by an attractive $\boldsymbol{U_{att}}$ and a repulsive $\boldsymbol{U_{rep}}$ component. The attractive component is responsible for pushing an object towards a goal, while the repulsive component pushes the object away from obstacles. The total APF, $\boldsymbol{U_{tot}}$ can then be denoted as:

$$\boldsymbol{U_{tot}} = \boldsymbol{U_{att}} + \boldsymbol{U_{rep}}. \tag{2.11}$$

The repulsive force is calculated as a function depending on the distance $d_{obs} > 0$ to an obstacle and an angle $0 \leq \theta_{obs} \leq 2\pi$ between the obstacle and the vessel. The distance d_{obs} and the angle θ_{obs} are calculated as:

$$d_{obs} = \sqrt{(x_{obs} - x_{os})^2 + (y_{obs} - y_{os})^2} \tag{2.12}$$

$$\theta_{obs} = arctan2(y_{obs} - y_{os}, x_{obs} - x_{os}) \tag{2.13}$$

where (x_{obs}, y_{obs}) is the position of the obstacles, and (x_{os}, y_{os}) is the position of the OS. The repulsive force from each obstacle is calculated as:

$$\boldsymbol{U_{obs}} = \begin{cases} k_{rep}(s_{rep} + r_{rep} - d_{obs}) \begin{bmatrix} cos(\theta_{obs}) \\ sin(\theta_{obs}) \end{bmatrix}, & \text{if } d_{obs} < r_{rep} + s_{rep} \\ 0, & else \end{cases} \tag{2.14}$$

where the variables $s_{rep} + r_{rep} > 0$ represent a safe distance from the obstacle, while $k_{rep} < 0$ is the repulsion parameter, s_{rep} and r_{rep} are also tuning parameters. Here, θ_{obs} defines the direction of the repulsive force. Assuming $n > 0$ obstacles, $\boldsymbol{U_{rep}}$ is the sum of the repulsive field of all obstacles

$$\boldsymbol{U_{rep}} = \sum_{obs=1}^{n} \boldsymbol{U_{obs,n}}. \tag{2.15}$$

The attractive field is calculated as a function function depending on the angle θ_{goal} calculated as

$$\theta_{goal} = arctan2(y_{goal} - y_{os}, x_{goal} - x_{os}), \tag{2.16}$$

where (x_{goal}, y_{goal}) is the position of the goal. The attractive field is further calculated as:

$$\boldsymbol{U_{att}} = k_{goal} s_{goal} \begin{bmatrix} cos(\theta_{goal}) \\ sin(\theta_{goal}) \end{bmatrix} \tag{2.17}$$

where $k_{goal} > 0$ is an attraction parameter and $s_{goal} > 0$ is a tuning parameter.

2.3 COLREGs

The purpose of this thesis is to produce a COLAV method that is COLREGs-aware. Rules 13-15 are the primary rules that will be used. A visualization of these rules can be seen in Figure 2.3, where the own-ship (OS) can be seen in blue, and the target-ship (TS) in red. In the following section, a description of the relevant COLREGs rules are stated as in Cockcroft and Lameijer (2012).

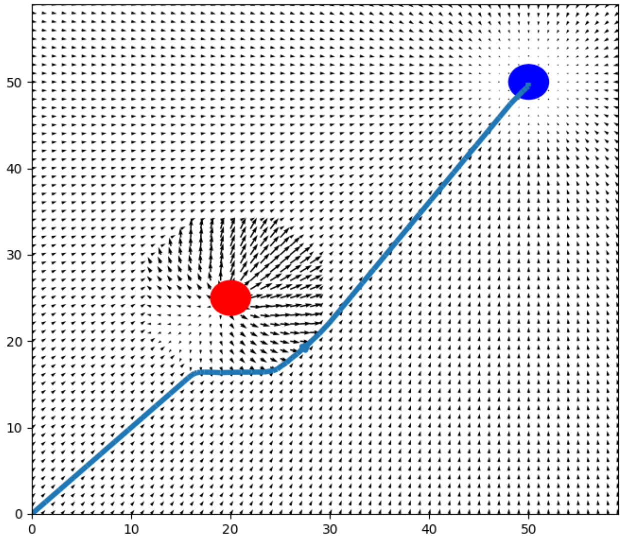

Figure 2.2: Illustration of an APF where the obstacle can be seen as the red circle, while the goal position is the blue circle. A path in blue navigates around the obstacle and towards the goal. The repulsive fields impact on the total potential filed can be seen around the obstacle.

2.3.1 Rule 13 overtaking

(a) Notwithstanding anything contained in the Rules of Part B, Sections I and II, any vessel overtaking any other shall keep out of the way of the vessel being overtaken.

(b) A vessel shall be deemed to be overtaking when coming up with another vessel from a direction more than 22.5 abaft her beam, that is, in such a position with reference to the vessel she is overtaking, that at night she would be able to see only the sternlight of that vessel but neither of her sidelights.

(c) When a vessel is in any doubt as to whether she is overtaking another, she shall assume that this is the case and act accordingly.

(d) Any subsequent alteration of the bearing between the two vessels shall not make the overtaking vessel a crossing vessel within the meaning of these Rules or relieve her of the duty of keeping clear of the overtaken vessel until she is finally past and clear.

2.3.2 Rule 14 head-on

(a) When two power-driven vessels are meeting on reciprocal or nearly reciprocal courses so as to involve risk of collision each shall alter her course to starboard so that each shall

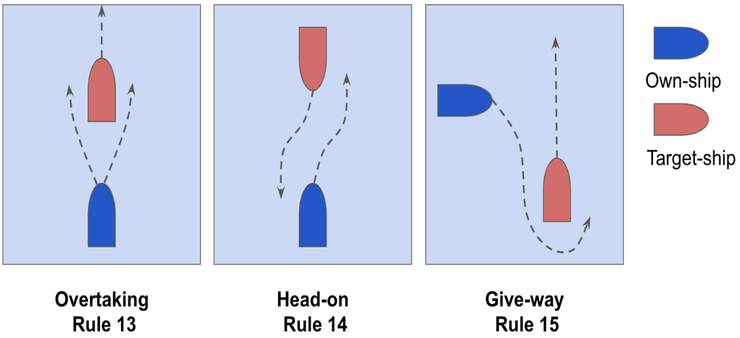

Figure 2.3: Considered COLREGs scenarios.

pass on the port side of the other.

(b) Such a situation shall be deemed to exist when a vessel sees the other ahead or nearly ahead and by night she could see the masthead lights of the other in line or nearly in a line and/or both sidelights and by day she observes the corresponding aspect of the other vessel.

(c) When a vessel is in any doubt as to whether such a situation exists she shall assume that it does exist and act accordingly.

2.3.3 Rule 15 give-way

When two power-driven vessels are crossing so as to involve risk of collision, the vessel which has the other on her own starboard side shall keep out of the way and shall, if the circumstances of the case admit, avoid crossing ahead of the other vessel.

Comment: Crossing situation shall be deemed to exist when a vessel is approaching the other vessel from a direction right ahead to 112,5 on any side of the vessel except when vessels are meeting on reciprocal or nearly reciprocal courses. In crossing situation at night a vessel would be able to see only green or red sidelight and masthead light (s) of the other vessel.

2.4 COLREGs classifier

As in the specialization project the method presented in Thyri (2021) is used as a COLREGs classifier. The following information is taken from the specialization project Kirkerud (2021): *It uses the position and velocity of the OS relative to the TS to determine which COLREGs rules are applicable. Figure 2.4 visualizes how the relationship translates into different rules, where the different segments stand for:*

- *Overtaking (OT): Rule 13*

- *Head-on (HO): Rule 14*
- *Give-way (GW): Rule 15*
- *Stand-on (SO): Rule 17*
- *Safe (SF): No rules apply.*

Rule 17, stand-on states that one of the vessels should stay out of the way while the other keeps her course and speed. The latter vessel could however take evasive action if the other vessel does not keep out of the way.

The OS can be seen in the middle of Figure 2.4, where each segment of its circle represent the window of one classification rule. The circles surrounding the OS represents the TS. The TS is divided into segments of different layers. These layers represent the relative velocity between the OS and TS, the inner represent a situation where the range between the TS and OS is increasing, while the outer represent a situation where the range is decreasing. The TS are also divided into segments which represents it's heading.

It is possible to classify the situation into a COLREGs rule by first finding the target ship region (TSR) by:

$$\psi_{TSR} = \psi_{ts} - \psi_{os} - \varphi_{ts} \tag{2.18}$$

where ψ_{ts} *is the bearing of the TS,* ψ_{os} *is the bearing of the OS, and* φ_{ts} *is found by:*

$$\varphi_{ts} = arctan2(y_{os} - y_{ts}, x_{os} - x_{ts}). \tag{2.19}$$

The correct TSR is then found using ψ_{ts} *together with* θ_1 *and* θ_2*.*

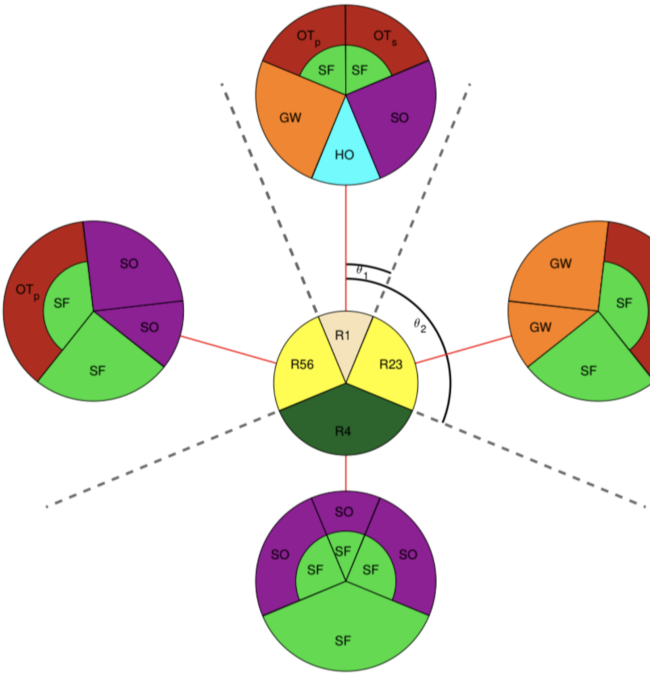

Figure 2.4: Illustration of the COLREGs classifier. Courtesy of Thyri (2021).

Chapter 3

Encounter-specific Artificial potential fields

In this chapter, the method proposed for COLREGs-compliant maneuvering and COLAV is presented in detail. First, situational awareness, which is how the vessels interpret the knowledge about the environment, is proposed. Then, the target ship domain, which is a domain assigned to each TS, is presented. The domain is specific to the COLREGs encounter type. Lastly the mechanism for calculating the APF and the associated reference signals are presented.

3.1 Situational awareness

Situational awareness for this COLAV method is divided into two parts. First a method for evaluating the risk of collision, then a COLREGs interpreter. The method used to evaluate the risk of collision is based on the *Safe passage circle and closest point of approach* method from Kufoalor et al. (2018). While the COLREGs interpreter is based on the classifier from Section 2.4.

3.1.1 *Safe passage circle and closest point of approach*

An OS is navigating in an environment with the presence of a TS. Both vessels are assumed to navigate with a constant velocity. To evaluate the risk of collision the distance between the vessels at CPA, $d^{CPA}_{OS,TS}$ is compared to the desired minimum distance between the vessels at CPA, $d^{min}_{OS,TS}$. First the time at which the distance between the OS and TS is minimum, $t^{CPA}_{OS,TS}$ is calculated by:

$$t^{CPA}_{OS,TS} = \begin{cases} \frac{(\boldsymbol{\rho}_{ts}-\boldsymbol{\rho}_{os})\cdot(\boldsymbol{v}_{os}-\boldsymbol{v}_{ts})}{\|\boldsymbol{v}_{os}-\boldsymbol{v}_{ts}\|^2}, & \text{if } \|\boldsymbol{v}_{os}-\boldsymbol{v}_{ts}\| > 0 \\ 0, & else \end{cases} \tag{3.1}$$

where $\boldsymbol{\rho_{os}}$ and $\boldsymbol{\rho_{ts}}$ are the positions of the OS and the TS, respectively, and $\boldsymbol{v_{os}}$ and $\boldsymbol{v_{ts}}$ are the vessels velocity in the inertial frame. Furthermore $d^{CPA}_{OS,TS}$ at $t^{CPA}_{OS,TS}$ is found as

$$d^{CPA}_{OS,TS} = \left\| (\boldsymbol{\rho_{os}} + t^{CPA}_{OS,TS}\boldsymbol{v_{os}}) - (\boldsymbol{\rho_{ts}} + t^{CPA}_{OS,TS}\boldsymbol{v_{ts}}) \right\|, \tag{3.2}$$

where $d^{CPA}_{OS,TS} < d^{min}_{OS,TS}$ would imply that the OS will collide with the TS.

3.1.2 COLREGs classifier

If a collision is detected, the situation must be categorized for the different COLREGs rules. This is done using the method presented in Section 2.4.

3.2 Target ship domain

In this section, the design of the target ship domains assigned to each TS are presented. Figures 3.2-3.3 show a visualization of how the different target ship domains are depending on the situations. Generally for the figures are that the OS can be seen in blue and the TS in red. The TS bearing is given by χ_{ts}, and φ_{ts} is the direction of the line-of-sight vector between OS and TS. Furthermore the deflection angle α_{def} is the deflection between the target ship domain line and the line-of-sight vector. A point $\boldsymbol{L}$ is set on the line-of-sight vector, with distance $l > 0$ from the TS. φ_{ts} is found by:

$$\varphi_{ts} = arctan2(y_{os} - y_{ts}, x_{os} - x_{ts}), \tag{3.3}$$

and the point $\boldsymbol{L}$ is found as:

$$\boldsymbol{L} = \boldsymbol{\rho_{ts}} + l \begin{bmatrix} cos(\varphi_{ts}) \\ sin(\varphi_{ts}) \end{bmatrix}. \tag{3.4}$$

The end points of the target ship domain, $\boldsymbol{L}_{start}$ and $\boldsymbol{L}_{end}$ are calculated as:

$$\boldsymbol{L}_{start} = \boldsymbol{L} - \boldsymbol{L}_{start} \begin{bmatrix} cos(\varphi_{ts} + \alpha_{def}) \\ sin(\varphi_{ts} + \alpha_{def}) \end{bmatrix}, \tag{3.5}$$

$$\boldsymbol{L}_{end} = \boldsymbol{L} + \boldsymbol{L}_{end} \begin{bmatrix} cos(\varphi_{ts} + \alpha_{def}) \\ sin(\varphi_{ts} + \alpha_{def}) \end{bmatrix}, \tag{3.6}$$

where $\boldsymbol{L}_{start}$ and $\boldsymbol{L}_{end}$ is the distance from $\boldsymbol{L}$ to the endpoints of the target ship domain. These distances are calculated as:

$$\boldsymbol{L}_{start} = \|\boldsymbol{L} - \boldsymbol{\rho}_{os}\| + \lambda_{start}, \tag{3.7}$$

$$\boldsymbol{L}_{end} = \|\boldsymbol{L} - \boldsymbol{\rho}_{ts}\| + \lambda_{end}, \tag{3.8}$$

where $\lambda_{start} > 0$ and $\lambda_{end} > 0$ are variables that offers an offset, such that $\|\boldsymbol{L}_{start} - \boldsymbol{L}\| > \|\boldsymbol{L} - \boldsymbol{\rho}_{os}\|$ and $\|\boldsymbol{L}_{end} - \boldsymbol{L}\| > \|\boldsymbol{L} - \boldsymbol{\rho}_{ts}\|$. This is important as it minimizes the risk of the OS crossing around $\boldsymbol{L}_{start}$, or pass between the domain and $\boldsymbol{L}_{end}$.

The different COLREGs situations will produce different target ship domains, making it beneficial to configure these situation differently.

3.2.1 Head-on

In Figure 3.1, a visualization of the target ship domain in a head-on situation is presented. In HO encounters, the deflection angle α_{def}, must be chosen such that when the OS approaches the domain, its natural way of deflection corresponds to a starboard maneuver. To ensure this, the deflection angle should be chosen such that $0 < \alpha_{def} < \psi_{os} + \pi$. To ensure that $\boldsymbol{L}_{end}$ is on the port side of the TS, the deflection angle must also satisfy $0 < \alpha_{def} < \psi_{ts} + \pi$. In general, the choice of the deflection angle α_{def}, defines how aggressive the OS will avoid the TS. A higher value, will create a domain that moves more across in front of the OS, and lead to a more aggressive course correction when the OS comes into contact with the domain.

The variable $l > 0$, defines the distance between $\boldsymbol{\rho}_{ts}$ and $\boldsymbol{L}$. This variable influences the minimum distance the OS will pass the TS with. The distance l, together with α_{def} also influence at what time the OS will interact with the target ship domain. By having a low value for α_{def} the point $\boldsymbol{L}_{start}$ will be closer to the OS, and the OS will interact with the target ship domain earlier than a high value for α_{def}. A high value for l will also cause an earlier interaction with the target ship domain, than a low value.

3.2.2 Overtaking

In Figure 3.2, a visualization of the target ship domain in a overtaking situation is presented. As the OS can overtake on either of the sides of the TS, a visualization of the target ship domain for both of these situations are given. In Figure 3.2a, the OS wants to perform an overtaking maneuver, and since the TS is crossing in front of the OS, it is natural that the OS will perform the overtaking maneuver on the port side of the TS. In such a situation the deflection angle must be chosen such that when the OS approach the domain, its deflection corresponds to a port side maneuver. To obtain this, the deflection angle must satisfy $3\pi/2 + \psi_{os} < \alpha_{def} < 2\pi$. This also ensure that $\boldsymbol{L}_{end}$ is on the port side of the TS and $\boldsymbol{L}_{start}$ is on the starboard side of the OS. The parameter α_{def} also impact when the OS come into contact with the domain. A higher deflection angle will lead to an earlier impact with the domain, as $\boldsymbol{L}_{start}$ is closer to the OS. A higher value will also

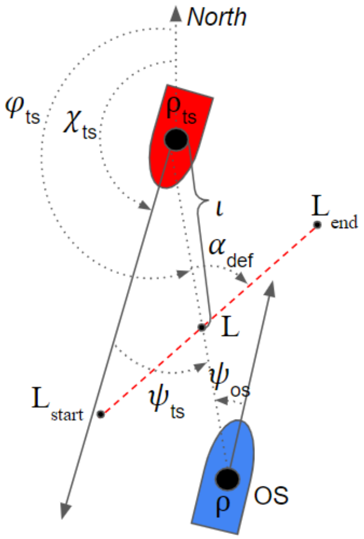

Figure 3.1: Target ship domain for a head-on encounter.

lead to less of a course correction, as the domain will be more parallel to the line-of-sight vector between the OS and the TS.

The length $l > 0$ decides the distance between the $\boldsymbol{L}$ and the TS. And together with α_{def} decides both how far away the TS the OS passes and at what time the OS comes into contact with the domain. A high deflection angle will cause the point $\boldsymbol{L}_{end}$ to be closer and lead more towards the TS. And a lower l will move the entire domain closer to the TS.

In Figure 3.2b, the TS is heading away from the OS, making it natural to perform the overtake maneuver on the starboard side of the TS. In such a situation the deflection angle must be chosen such that when the OS approach the domain, its the deflection corresponds to a starboard maneuver. To obtain this, the deflection angle must satisfy $0 < \alpha_{def} < \pi/2 + \psi_{os}$. This also ensure that $\boldsymbol{L}_{end}$ is on the starboard side of the TS and $\boldsymbol{L}_{start}$ is on the port side of the OS. The parameter α_{def} also impacts when the OS comes into contact with the domain. A higher deflection angle will lead to an later impact with the domain, as $\boldsymbol{L}_{start}$ is further away from the OS. A higher value will also lead to a more aggressive course correction, as the domain will be more across to the line-of-sight vector between the OS and the TS.

The parameter l together with α_{def} decides both how far away the TS the OS passes and at what time the OS comes into contact with the domain. A low deflection angle will cause the point $\boldsymbol{L}_{end}$ to be closer and lead more towards the TS. And a higher l will move the entire domain closer to the TS.

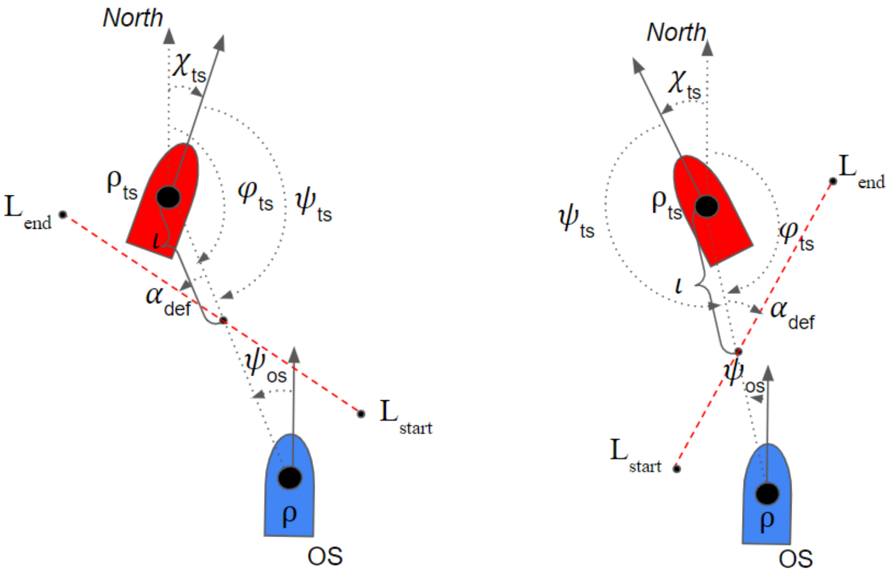

(a) Overtake port side

(b) Overtake starboard side

Figure 3.2: The target ship domains for a overtake situation where the vessel can overtake on either of the sides of the TS.

3.2.3 Give-way

In Figure 3.3, a visualization of the target ship domain in a give-way scenario is presented. In a give-way situation the OS must make a starboard maneuver, passing behind the TS. The deflection angle α_{def}, must be chosen such that when the OS approaches the domain, its natural way of deflection corresponds to a starboard maneuver. To ensure this, the deflection angle must be chosen such that $0 < \alpha_{def} < \pi/2 - \psi_{os}$. The deflection angle α_{def}, decides how aggressive the evasive maneuver will be. A higher value would lead to a domain that moves more across the line-of-sight vector between the TS and the OS.

The length length $l > 0$, decides the distance between $\boldsymbol{L}$ and the TS. Together with α_{def} they define at what time the OS comes into contact with the domain. A smaller value for the α_{def} will cause the point $\boldsymbol{L}_{start}$ to be closer to the OS, as well as a larger value for l will cause the point $\boldsymbol{L}$ to be closer to the OS. Both of these effects will cause the OS to interact with the domain at an earlier time. The values also have an impact on how close the OS will pass the TS. Where a low value for the deflection angle and a low value for l will cause the point $\boldsymbol{L}_{end}$ to be closer to the TS, and OS will pass closer to the TS.

3.3 Artificial potential field

The APF contains as defined in Section 2.2, an attractive and an repulsive component. In this section, a detailed description of how these components are calculated, along with the

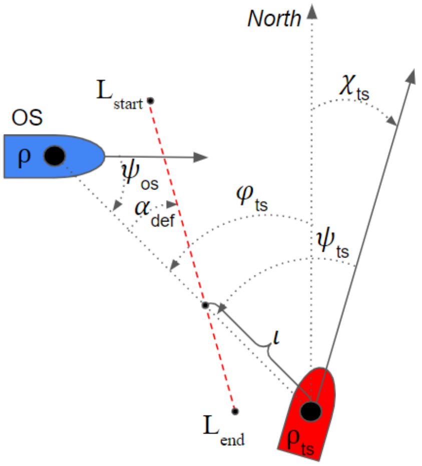

Figure 3.3: Target ship domain for a give-way situation.

method for calculating the reference signals for collision free maneuvering of the OS are presented.

3.3.1 Attractive force

The attractive force is responsible for pushing the OS towards a goal position $\boldsymbol{\rho_{goal}}$. The line-of-sight (LOS) guidance method is responsible for finding this goal position. Where, $\boldsymbol{\rho_{goal}}$ is found as a point on the nominal trajectory. With the OS in position $\boldsymbol{\rho_{os}}$, and a point on the trajectory at time t denoted as $\boldsymbol{\rho_{traj(t)}}$. The distance between $\boldsymbol{\rho_{os}}$ and $\boldsymbol{\rho_{traj(t)}}$ denoted $d_{os,traj(t)} \geq 0$, is found as,

$$d_{os,traj(t)} = \left\| \boldsymbol{\rho_{os}} - \boldsymbol{\rho_{traj(t)}} \right\| . \tag{3.9}$$

The relative bearing $\psi_{traj(t)} \in [-\pi, \pi]$, between $\boldsymbol{\rho_{os}}$ and $\boldsymbol{\rho_{traj(t)}}$ is given by

$$\psi_{traj(t)} = atan2(y_{os} - y_{traj(t)}, x_{os} - x_{traj(t)}) - \varphi_{traj(t)}, \tag{3.10}$$

where y_{os} and x_{os} are the y and x position of the OS in $\boldsymbol{\rho_{os}}$, and $y_{traj(t)}$ and $x_{traj(t)}$ are the y and x position of the goal in $\boldsymbol{\rho_{traj(t)}}$, and $\varphi_{traj(t)}$ is the trajectory bearing at time t. To ensure that $\boldsymbol{\rho_{goal}}$ is a point in front of the OS, and with reasonable distance from $\boldsymbol{\rho_{os}}$ it is chosen as,

$$\boldsymbol{\rho_{goal}} = \underset{\forall \boldsymbol{\rho_{traj(t)}} \in \boldsymbol{P_{traj}}}{\arg\min} \{d_{os,traj(t)}(\boldsymbol{\rho_{traj(t)}}) | d_{os,traj(t)} \geq d_{os,traj}^{min} \; and - \pi/2 \leq \psi_{traj(t)} \leq \pi/2\}, \tag{3.11}$$

where $\boldsymbol{P_{traj}} \in \boldsymbol{R}^{N \times 2}$ is a matrix containing N position points in the trajectory.

When $\boldsymbol{\rho_{goal}}$ is set, the attractive force can be calculated. This is done by first calculating θ_{goal} with (2.16). The final attractive force $\boldsymbol{U_{att}}$ can then be calculated with (2.17), where the parameters $k_{goal} > 0$ and $s_{goal} > 0$ decide the strength of attractive force. With high values, the attractive force will be greater, and the attractive force will have a greater influence over the total potential force. Choosing the correct parameters are therefore highly coupled with the choice of the parameters for the repulsive force.

3.3.2 Repulsive force

The repulsive force is responsible for pushing the OS away from obstacles. In the proposed method, the obstacles are divided into two groups; TSs and stationary obstacles.

Repulsive force from target ships

The repulsive force form the TSs are calculated with respect to the target ship domain defined in Section 3.2. A line is constructed through n_{points} points along the line representing the target ship domain. Each of these points are considered an obstacle when creating the repulsive force. The choice of n_{points} determines the density of the obstacles, and will further have an impact on the resulting repulsive force. One option is to make the density of obstacles constant. This can be done by setting n_{points} as a parameter dependent on the length of the target ship domain line. Hence,

$$n_{points} = \rho_{obs}(\boldsymbol{L}_{start} + \boldsymbol{L}_{end}) \tag{3.12}$$

where $\rho_{obs} > 0$, is a parameter that decides the density of the obstacles. The line ends up as a matrix $\boldsymbol{P}_{ts,obs} \in \boldsymbol{R}^{n_{points} \times 2}$.

The line from the target ship domain also has a direction φ_{line} from $\boldsymbol{L}_{start}$ to $\boldsymbol{L}_{end}$ relative to North, found as

$$\varphi_{line} = \pi - (\varphi_{ts} + \alpha_{def}). \tag{3.13}$$

The repulsive force can then be calculated from $\boldsymbol{P}_{ts,obs}$ and φ_{line}. The force from each of the obstacles are calculated from (2.14), where $\theta_{obs} = \varphi_{line}$ and d_{obs} is calculated as in (2.12). The points x_{obs} and y_{obs} are the position of the respective obstacle from $\boldsymbol{P}_{ts,obs}$. The parameters k_{rep}, s_{rep} and r_{rep} are tunable parameters, that have affect on the strength of the repulsive forces from the obstacles. The parameters s_{rep} and r_{rep} decides how much the strength of the repulsive force should depend on d_{obs}. A higher value for s_{rep} and r_{rep} will result in a repulsive force which is less dependent on d_{obs}. This would cause the repulsive force to be more constant around the obstacles, instead of gradually becoming greater towards the center of the obstacle. A more gradually repulsive force is desired, as this will cause a smoother navigation when the OS is in contact with the target ship domain. k_{rep} are the main contributor to the strength of the repulsive force, and highly dependent on n_{points}. With a high density of obstacles k_{rep} should be lower. As the OS comes into contact with the target ship domain, if the density is high more obstacles will have an impact on the total force.

When a repulsive force is calculated for each of the dynamic obstacles, the total repulsive force is calculated by (2.15).

Repulsive force from stationary obstacles

The stationary obstacles are constructed as a polygon, where the vertices are set. A line segment is constructed between each of the vertices, by setting a unique $n_{points,segment} > 0$ number of points along each of the line segments, calculated by,

$$n_{points,segment} = \rho_{obs,stationary}(\boldsymbol{Q}_{start,segment} + \boldsymbol{Q}_{end,segment}), \tag{3.14}$$

where $\boldsymbol{Q}_{start,segment}$ and $\boldsymbol{Q}_{end,segment}$ are the start and end point of each of the segments. The density variable $\rho_{obs,stationary}$, is set constant for all the segments, such that the density for all the segments are the same. The points along the segments are referred to as an obstacle, and combined into the matrix $\boldsymbol{P}_{obs} \in \boldsymbol{R}^{n_{obs} \times 2}$, where $n_{obs} > 0$ are the sum of $n_{points,segment}$ for all the segments. A repulsive force is then assigned to each of these obstacles independently. The repulsive force is calculated as in (2.14), where θ_{obs} is calculated as in (2.13) and d_{obs} is calculated as in (2.12). This creates a repulsive force which points towards the OS. The variables k_{rep}, s_{rep} and r_{rep} work very much the same as for the *Repulsive force from target ships*. The density of the obstacles $\rho_{obs,stationary}$ influence the choice of k_{rep}, s_{rep} and r_{rep}, where a higher density would cause the need for lower values for the other parameters. The parameters $\rho_{obs,stationary}, k_{rep}$, s_{rep} and r_{rep} should be chosen such that the total repulsive force at the position of an obstacle, contributes much more to the total force, than the attractive force.

When each of the obstacles has been given a repulsive force, the total repulsive force is calculated as in (2.15).

3.3.3 Total force

The total force is calculated as the sum of the repulsive and attractive forces as in (2.11), where U_{rep} is the sum of the repulsive force from the stationary obstacles and the repulsive force from the target ships.

3.4 Reference filter

The reference filter is responsible for converting the total force from the APF, into positional, heading and velocity references. The total force from the APF consist of two forces, one in the X direction denoted, δ_x, and one in Y direction denoted, δ_y. A desired heading can be calculated from these forces as,

$$\psi_d = atan2(\delta_y, \delta_x). \tag{3.15}$$

From ψ_d the desired velocity can then be found by:

$$\begin{bmatrix} \dot{X}_d \\ \dot{Y}_d \end{bmatrix} = V \begin{bmatrix} cos(\psi_d) \\ sin(\psi_d) \end{bmatrix}. \tag{3.16}$$

Here, $V > 0$ is the absolute desired speed. The desired heading rate $r = 0$, since the milliAmpere vessel model used in the simulations is very sensitive in heading. Finally the desired positions can be calculated as:

$$\begin{bmatrix} X_d \\ Y_d \end{bmatrix} = \begin{bmatrix} X_{os} \\ Y_{os} \end{bmatrix} + \begin{bmatrix} \dot{X}_d \\ \dot{Y}_d \end{bmatrix} dt, \tag{3.17}$$

where $[X_{os}, Y_{os}]^T = \boldsymbol{\rho}_{os}$ is the current position of the vessel and $dt > 0$ is a variable which decides how far away the desired positions should be from the current position and should be chosen to match the run-period of the propose APF algorithm to ensure that the velocity and position references correspond.

Chapter 4

Simulation results

4.1 Simulator design

A Python simulator was developed for this project. The Numpy library was used to optimize the run-time, by compiling the vector and matrix calculations into C. The simulator developed for this project enables the opportunity to test and verify the performance of reactive COLAV methods. The simulator is designed with many modules, representing the different parts of the autonomous pipeline. A visualization of the pipeline can be seen in Figure 4.1.

4.1.1 Situational awareness

The situational awareness module is responsible for determining the chance of collision, and categorize these situations into COLREGs rules. Determining the chance of collision is based on the *Safe passage circle and closest point of approach* method from Kufoalor et al. (2018). The method is explained detail in Section 3.1.1, and the python implementation can be seen in Appendix A.1. The criteria for classifying an encounter as a collision encounter is $d^{CPA}_{OS,TS} < d^{min}_{OS,TS}$. In the simulations that follow, $d^{min}_{OS,TS} = 30$. Implying that if the vessels are closer than 30 meters from each other at the CPA, it is classified as an encounter with risk of collision.

When an encounter has a risk of collision it is categorized according to the COLREGs rules. Here, the classifier from Section 2.4 is implemented by first finding the correct bearing sector and then the correct situation sector. The bearing sector and the situation sector are then used to lookup the correlating COLREGs situation.

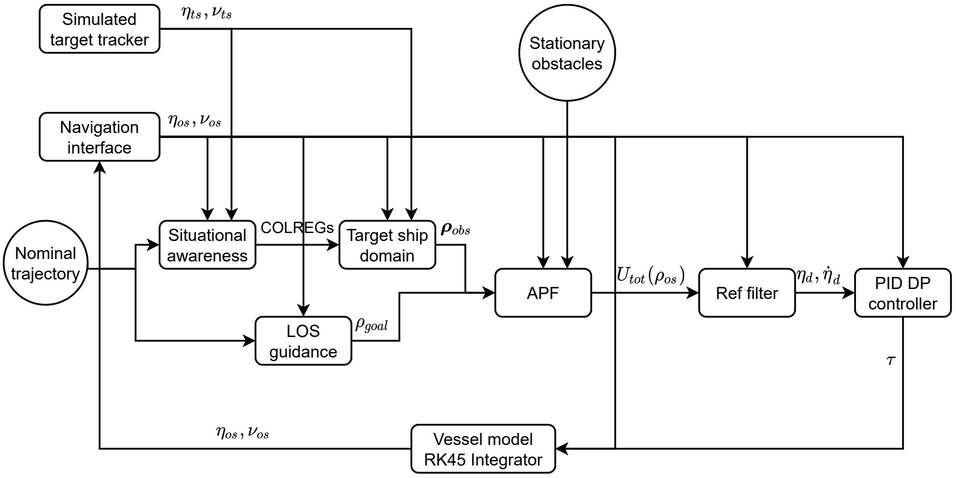

Figure 4.1: Autonomous navigation with COLAV pipeline for the simulator.

4.1.2 Target ship domain

When a collision is detected and categorized, the target ship domain module is responsible for creating a COLREGs specific domain which makes the OS navigate in accordance to the COLREGs rules. The target ship domain module use the states of the OS and the TS, to correctly place the domain. The domain is produced as in Section 3, where points are set along the domain, together with the direction the repulsive forces of the APF should point.

Head-on

The HO specific target ship domain is described in Section 3.2.1. The parameters used in the simulations can be seen in Table 4.1. These parameters were found after some tuning from numerical simulations, under different HO situations. As the method proposed works when a collision is immediate, it can be assumed that there is limited space between the OS and the TS at the initialization phase. The distances between the vessel at the initialization phase is assumed to be greater than 100 meters. The distance l, is set to 75 meters, such that it is less than the distance between the vessels at initialization, which ensures that $\boldsymbol{L}$ is between the OS and the TS at the line-of-sight vector. Both λ_{start} and λ_{end} are set to 20 meters, as this ensures enough offset such that the vessels do not cross above $\boldsymbol{L}_{start}$ or between $\boldsymbol{L}_{end}$ and the TS. Lastly, $\alpha_{def} = 9\pi/10$, a choice which required some tuning. This choice resulted in decent maneuvering from the OS, for different HO situation configurations.

Overtake

The OT specific target ship domain is described in Section 3.2.2, and the parameters used in the simulations can be seen in tables 4.2 and 4.3. The target ship domain is specific for

Parameter	Value	Unit
α_{def}	$9\pi/10$	rad
l	75	m
λ_{start}	20	m
λ_{end}	20	m

Table 4.1: Parameters used in the simulations for the target ship domain in an head-on scenario.

OT on starboard side and OT on port side, where the target ship domain for overtaking on the starboard side is symmetric to the the target ship domain for overtaking on the port side. The parameters used for the target ship domain for OT on starboard side was fist determined. This was done by numerical simulations, where different parameters were tested, to achieve optimal maneuvering. As the proposed method proposed works when a collision is immediate, it can be assumed that there is limited space between the OS and the TS at the initialization phase. The distances between the vessel at the initialization phase is however assumed to be greater than 100 meter. The distance l is set to 75 meters, such that it is less than the distance between the vessels at initialization, which ensures that L is between the OS and the TS at the line-of-sight vector. Both λ_{start} and λ_{end} are set to 20 meters, as this ensures enough offset such that the vessels does not cross above L_{start} or between L_{end} and the TS. Lastly, $\alpha_{def} = 6\pi/20$. The parameter required some tuning, to achieve the desired behavior. This choice resulted in decent maneuvering from the OS, for different HO situation configurations.

For overtaking on the port side of the TS, the parameters l, λ_{start} and λ_{end} were set as the same as the parameters used for overtaking on the starboard side of the TS. This is because the arguments for choosing these parameters at those values are the same for overtaking on the starboard side and the port side. The deflection angle that corresponds to the symmetric target ship domain to the overtaking on the port side is $\alpha_{def} = 34\pi/20$.

Parameter	Value	Unit
α_{def}	$34\pi/20$	rad
l	75	m
λ_{start}	20	m
λ_{end}	20	m

Table 4.2: Parameters used in the simulations for the target ship domain in an overtaking on the port side scenario.

Give-way

The HO specific target ship domain is described in Section 3.2.3. The parameters used in the simulations can be seen in Table 4.3. These parameters were found after some tuning from numerical simulations, under different GW situations. The proposed method works when a collision is immediate, it can be assumed that there are limited space between the OS and the TS at the initialization phase. The distances between the vessel at the initialization phase are assumed to be greater than 100 meters. The distance l is set to 75 meters,

Parameter	Value	Unit
α_{def}	$6\pi/20$	rad
l	75	m
λ_{start}	20	m
λ_{end}	20	m

Table 4.3: Parameters used in the simulations for the target ship domain in an overtaking on the starboard side scenario.

such that it is less than the distance between the vessels at initialization, which ensures that L is between the OS and the TS at the line-of-sight vector. Both λ_{start} and λ_{end} are set to 20 meters, as this ensures enough offset such that the vessels does not cross above L_{start} or between L_{end} and the TS. Lastly $\alpha_{def} = \pi/2.2$, a parameter which required some tuning. This choice resulted in decent maneuvering from the OS, for different GW situation configurations.

Parameter	Value	Unit
α_{def}	$\pi/2.2$	rad
l	75	m
λ_{start}	20	m
λ_{end}	20	m

Table 4.4: Parameters used in the simulations for the target ship domain in a give-way scenario.

4.1.3 LOS guidance

The line-of-sight (LOS) guidance module is responsible for finding the goal position $\boldsymbol{\rho}_{goal}$ that the APF uses to create the attractive field. The method used to find this goal position is described in detail in Section 3.3.1, and the python implementation can be seen in Appendix A.2. The goal position is determined from the parameter $d_{os,traj}^{min}$. As previously stated the method works when collisions are immediate, and the vessels are also navigating in relatively confined waters. The choice of $d_{os,traj}^{min}$ will determine how fast the OS will converge towards the nominal trajectory, where a low value for $d_{os,traj}^{min}$ will result in quicker convergence. A higher choice of $d_{os,traj}^{min}$ will allow the OS to navigate further away from the nominal trajectory. After some numerical simulations with different values for $d_{os,traj}^{min}$, it was chosen to be 100 meters. This proved to give the OS enough room to navigate away from the nominal trajectory and it provided a nice convergence towards the nominal trajectory when the OS had performed an evasive maneuver.

4.1.4 Artificial potential field

The calculation of the APF is described in detail in Section 3.3. The choice of the parameters are all determined by numerical simulations under different situations. First, the parameters for the attractive force were determined, as presented in Table 4.5. By starting with setting the parameters for the attractive force, the focus would be on setting parameters for the repulsive force, such that they correspond nicely with the attractive force.

For the repulsive force for the TSs, the parameter $\boldsymbol{\rho}_{obs}$ which decides the density of the obstacles at the target ship domain was first chosen as $\boldsymbol{\rho}_{obs} = 1$. This means that there were 1 obstacle per meter on the target ship domain. An increase in density would not only have an impact on the tuning parameters, but also the run-time of the creation of the APF. The method has to loop through all the obstacles and calculate the repulsive force for them one by one, which is a slow process in python. The parameters k_{rep}, s_{rep} and r_{rep} where then chosen as presented in Table 4.6. Since r_{rep} defines the radius for the repulsive force for each obstacle it is determined first. A good radius proved to be $r_{rep} = 20$ meters, where the repulsive force from the target space domain then span to 20 meters on each side of it. Next the parameter s_{rep} is chosen as $s_{rep} = 1$. It is desirable to have a significantly stronger repulsive in the center of the obstacle, than around of it. Lastly, the parameter k_{rep} is chosen, and this is the primary tuning variable for the repulsive force. After testing the system with different values for k_{rep}, it landed on $k_{rep} = 0.5$. A smaller value would lead the repulsive force to be outweigh by the attractive field, causing the OS to make minimal maneuvering, while a large value would cause the OS to make a very dramatic maneuver.

Lastly the parameters used for the repulsive force for the stationary obstacles are determined. The parameters chosen can be seen in Table 4.7. The density of the stationary obstacles are as the density of the obstacles from the TSs set to 1 obstacle per meter. Where an increase in the density would both have an impact on the run-time of the algorithm, and the choice of the other parameters. The parameters k_{rep}, s_{rep} and r_{rep} are set such that the vessel must navigate away from the obstacle if it comes into contact with it. The radius r_{rep} is set to 10 meters, such that the vessel has 10 meters clearing to avoid the obstacle. And $s_{rep} = 3$, such that the repulsive force is dependent on the distance between the OS and the obstacle, but not too much. Lastly $k_{rep} = 0.7$, to provide enough repulsive force to ensure that the vessel does not come into contact with the obstacle.

Parameter	Value
k_{goal}	50
s_{goal}	1

Table 4.5: Parameters used in the simulations for creating the attractive force in the APF.

Parameter	Value
k_{rep}	0.5
s_{rep}	1
r_{rep}	20

Table 4.6: Parameters used in the simulations for creating the repulsive force for the TSs in the APF.

Parameter	Value
k_{rep}	0.7
s_{rep}	3
r_{rep}	10

Table 4.7: Parameters used in the simulations for creating the repulsive force for the stationary obstacles in the APF.

4.1.5 Reference filter

The reference filter is created as described in Section 3.4, and is responsible for creating positional, heading and velocity references that are used in the PID dynamic position (DP) controller. For the reference filter the absolute desired speed V is found as the absolute speed in the closest point on the nominal trajectory. And dt, which is the variable that decides the distance between the OS current position and the desired position. The value of dt is found through numerical simulations, where $dt = 6$, resulted in a nice behaviour from the OS.

4.1.6 PID DP controller

In this module, a PID DP controller with a 3-DOF vessel model is implemented to calculate the $\boldsymbol{\tau}$ that is needed for the OS to navigate from the current state to the desired state. The PID DP controller is developed by the milliAmpere team here at NTNU. The implementation of the part of the DP PID controller that calculates $\boldsymbol{\tau}$ is presented in Appendix A.3.

4.1.7 Vessel model RK45 integrator

The last module is responsible for updating the OS states with the 3-DOF kinetic vessel model from Section 2.1.2. Since the simulation environment is without influence of wind and waves the kinetics model can be simplified to:

$$\dot{\boldsymbol{\nu}} = \boldsymbol{M}^{-1}(\boldsymbol{\tau} - (\boldsymbol{C}(\boldsymbol{\nu}) + \boldsymbol{D}(\boldsymbol{\nu}))\boldsymbol{\nu}) \tag{4.1}$$

and the kinematics:

$$\dot{\boldsymbol{\eta}} = \boldsymbol{R}(\psi)\boldsymbol{\nu}, \tag{4.2}$$

where $\boldsymbol{R}(\psi) := \boldsymbol{R}_{z,\psi}$ still applies. By using a 4th order Runga-Kutta method to integrate over the model with the current state, a precise new state is found. The implementation of this is found in Appendix A.4

4.2 Simulated scenarios

In this section, the results from numerical simulations are presented. Four types of simulations are included in this report:

- Batches of simulations from simple single-vessel encounters in open waters, which are used to demonstrate the completeness and robustness of the proposed COLREGs-aware APFs.
- A varied set of more complex simulations that demonstrate the versatility of the method.
- Simulations that demonstrate the limitations of the method.
- Simulations comparing the proposed method to a standard APF method without COLREGs-aware APFs.

4.2.1 Batch plots

In the first results, multiple batch plots are presented. In these plots the OS is seen having a path parallel to the Y axis, starting at different points on the X axis. The TS approaches the OS path with a different attack angle in each of the individual plots to produce a specific COLREGs situation. Three situations are presented for each of the COLREGs rules, chosen to showcase the robustness of the proposed COLAV method.

Give-way situation with 90 degrees attack angle

In Figure 4.2, a batch plot of a give-way situation where the OS and the TS approach each other with an 90 degree attack angle is presented. It is clearly seen in the figure that the OS makes a starboard turn in order to give-way to the TS when a collision is detected. It can also be seen that the amount of starboard turn the OS makes, is dependent on the initial position of the OS relative to the TS. When the OS is starting at a higher position on the X axis the starboard turn are much larger than when it is starting at a lower X position. The starboard turn of the lower X positions are however stronger than simply following a minimum safe path, as the path can be seen overshooting the minimum safe path. This is considered good performance as is clearly signals to the TS that the OS is taking action to avoid collision.

Give-way situation with 120 degrees attack angle

In Figure 4.3, a batch plot of a give-way situation where the OS and the TS approach each other with an 120 degree attack angle is presented. The OS has give-way obligations, and should stay clear of the TS by making a starboard maneuver.With an higher attack angle than in Figure 4.2, it can be observed that the situation require less of a starboard turn to avoid the collision. The OS also overshoots the minimum safe path in this scenario, which is as stated earlier a good behaviour.

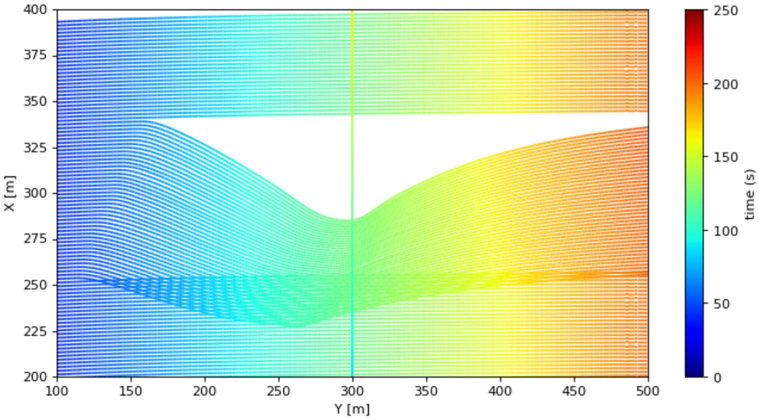

Figure 4.2: Batch plot of a give-way situation with 90 degrees attack angle.

Give-way situation with 60 degrees attack angle

In Figure 4.4, a batch plots similar to the previous two is presented. In this scenario the attack angle between the OS and the TS is however 60 degrees. As the ships approach with a shallower attack angle it is necessary for the OS to perform more of an aggressive starboard turn in order to avoid the collision. It can also be seen in the figure that the number of OS paths that are avoiding the collision are more than in the previous two scenarios, where the 120 degree attack angle scenario has the fewest.

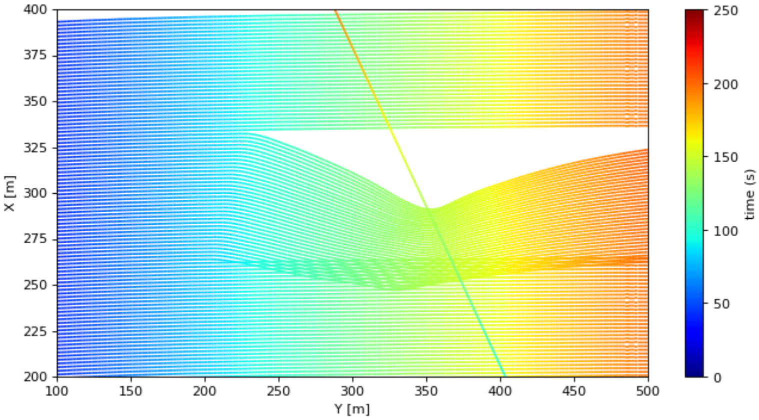

Figure 4.3: Batch plot of a give-way situation with 120 degrees attack angle.

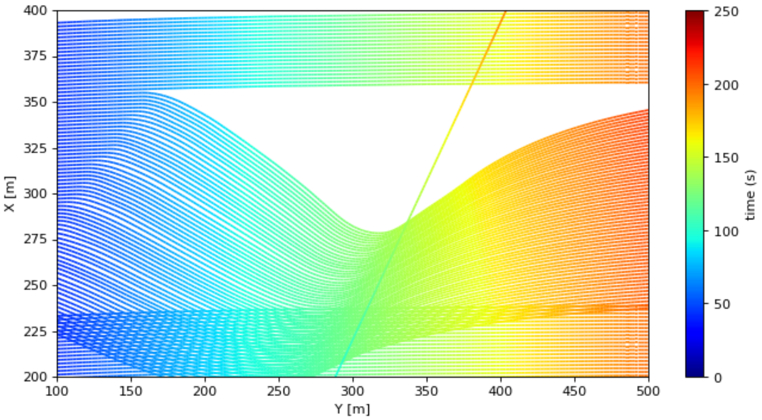

Figure 4.4: Batch plot of a give-way situation with 60 degrees attack angle.

Head-on situation with 180 degrees attack angle

In Figure 4.5, the TS is now following a path that runs right to left, creating a head-on situation with the OS. COLREGs deem that both vessels in a head-on situation should preform a starboard turn in order to avoid the collision. In the batch simulations presented here, the TS is however not maneuvering, but in stead keeping a constant velocity. From the figure it is clear that the OS performs a starboard turn in order to avoid the collision. The turn starts at a point and keeps going until the OS has passed the TS. When the OS has passed the TS it converges slowly towards the nominal path.

Head-on situation with 160 degrees attack angle

In Figure 4.6, the TS path is now rotated 20 degrees clockwise to create a head-on situation with an 160 degree attack angle between the OS and TS. The OS is clearly seen taking an evasive maneuver to the starboard side. The maneuver is however initiated much later than in the previous scenario, and also consist of a more aggressive starboard turn. The smaller attack angle in this scenario will create a shield which heading relative to the OS heading is smaller than in the previous scenario. The OS will approach a shield which leads to an aggressive starboard turn. And since the shield's heading relative to the OS heading is smaller, and the distance l from the TS to the shield is constant, it will take a longer time for the OS to come into contact with the shield.

Head-on situation with 200 degrees attack angle

In Figure 4.7, a batch plot of a head-on situation where the OS and the TS approach each other with a 200 degree attack angle is presented. The OS is seen performing a starboard turn in front of the TS avoiding the collision before it converges back to its original path. The OS navigates smoothly around the TS, with minimal changes to the heading.

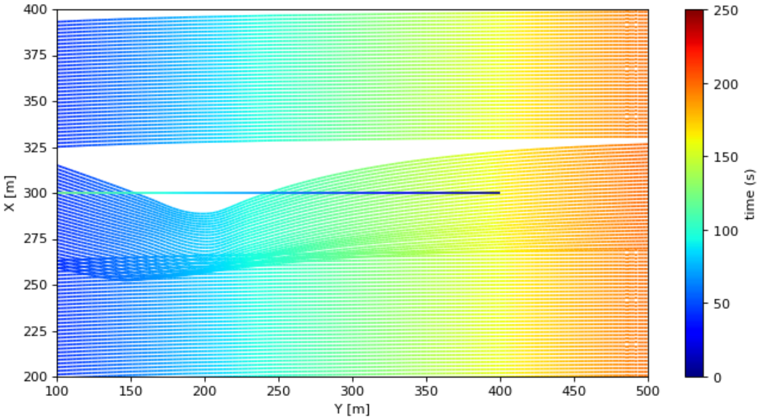

Figure 4.5: Batch plot of a head-on situation with 180 degrees attack angle.

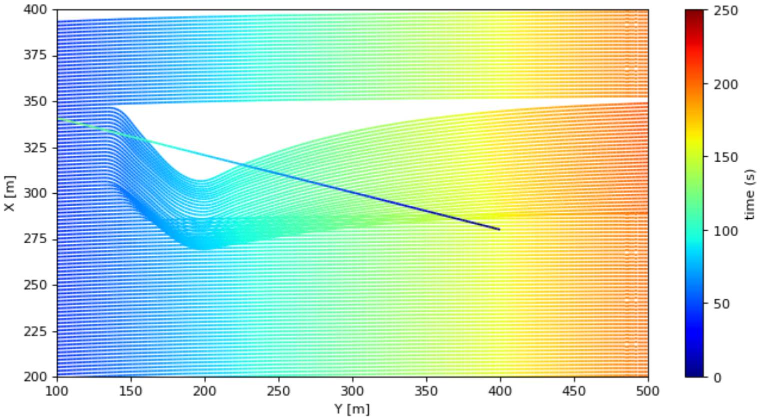

Figure 4.6: Batch plot of a head-on situation with 160 degrees attack angle.

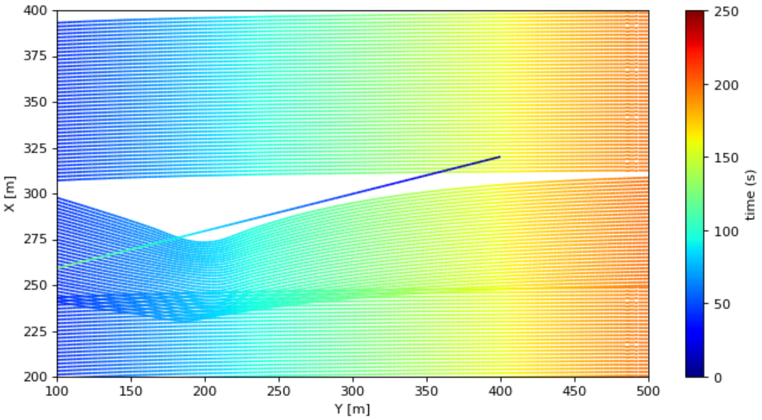

Figure 4.7: Batch plot of a head-on situation with 200 degrees attack angle.

Overtake situation with 0 degree attack angle

In Figure 4.8, the TS is seen navigating left to right at a lower velocity than the OS. This leads to an overtaking scenario where the OS can pass on the starboard or port side of the TS. The figure shows that the OS performs a starboard or port side turn dependent on how it is positioned relative to the TS. When the OS is above the TS on the X axis it does a port side turn, and when the OS is below the TS on the X axis it does a starboard turn. The OS performs a smooth turn, and navigates safely around the TS.

Overtake situation with 330 degree attack angle

In Figure 4.9, the TS path has been rotated 30 degrees counter clockwise creating an 330 degree attack angle between the OS and the TS. In this situation the OS makes a starboard turn passing behind the TS, before it converges towards its nominal path. It is also clear to see from the figure that the amount of starboard turn is much less for the OS paths that starts low on the X axis than those starting higher. This happens since the OS can take less of a starboard turn to avoid the collision. It is however also important that the starboard turn is strong enough to provide a clear signal to the TS that it has done an evasive maneuver.

Overtake situation with 30 degree attack angle

In Figure 4.10, the OS approach the TS with a 30 degree attack angle. This creates an opposite scenario as the previous one, where the OS now performs a port side turn to pass behind and on the port side of the TS. The general performance of the OS is however the same as the previous scenario. This is expected since the performance of port side turn should resemble the performance of the starboard turn.

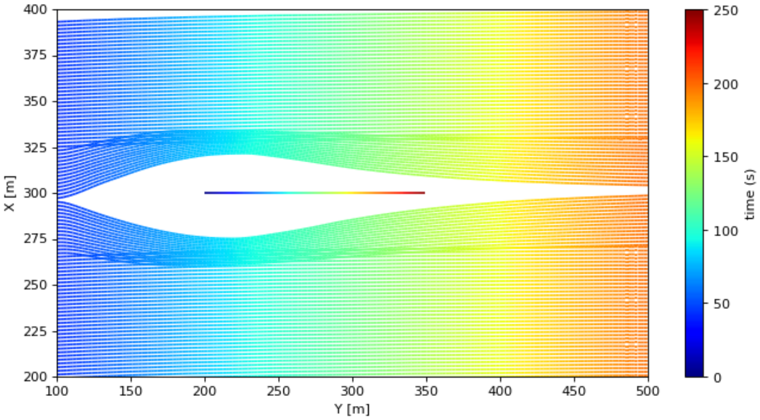

Figure 4.8: Batch plot of a overtake situation with 0 degree attack angle.

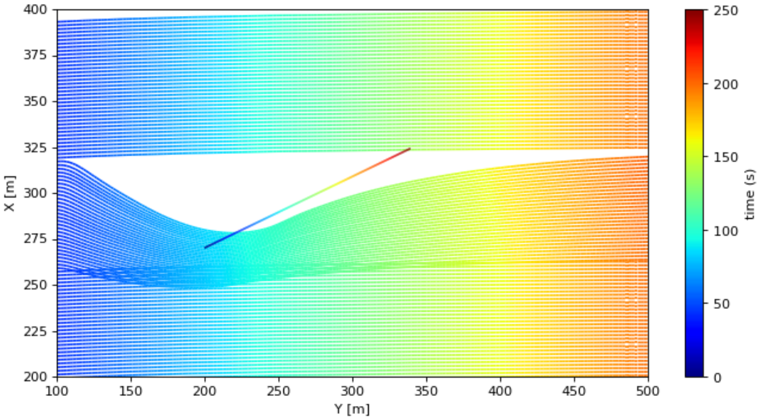

Figure 4.9: Batch plot of a overtake situation with 330 degree attack angle.

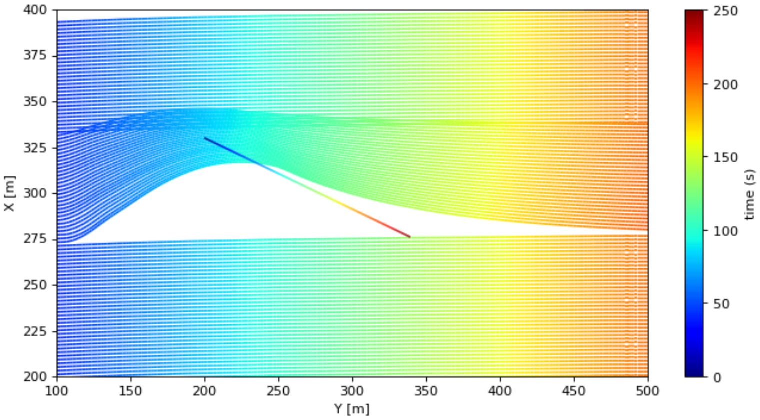

Figure 4.10: Batch plot of an overtake situation with 30 degree attack angle.

4.2.2 One-ship encounter with stationary obstacles

Three situations where the OS needs to perform an evasive action to avoid a collision with a TS under presence of some stationary obstacle such as land or shallow water are presented in this subsection. The nominal paths for both OS and TS are considered to be safe, such that the OS will only be in risk of crashing with a stationary obstacle if it deviates from the nominal path.

Overtake situation along land.

In Figure 4.11, the OS is denoted as Ship 1 and the TS is denoted as Ship 2. Both ships are keeping a path parallel to the Y axis, where Ship 2 holds a lower velocity than Ship 1. This creates an overtaking scenario. Ship 1 can then choose to pass on either of the sides of Ship 2. In this scenario Ship 1 is placed below Ship 2 on the X axis, and therefor choose to pass on the starboard side. A stationary obstacle is placed parallel to the paths, visualized as the tan area at the bottom of the figure. From the figure, Ship 1 can be seen taking the starboard turn to overtake Ship 2. When Ship 1 approach the stationary obstacle it corrects its course to go parallel to the stationary obstacle and keeps this course for a moment. It then starts to converge to its nominal path.

Give-way situation along land.

In Figure 4.12, two vessels Ship 1 the OS and Ship 2 the TS are visualized. Ship 1 has a nominal path parallel to the Y axis, going left to right, while Ship 2 has a nominal path parallel to the X axis, going upwards. The vessels are keeping the same speed. These nominal paths create a give-way situation, where Ship 1 must give-way to Ship 2. A stationary obstacle is also placed at the bottom left corner of the figure. When Ship 1 does a starboard turn to avoid the collision with Ship 2, it holds a path nearly parallel to the

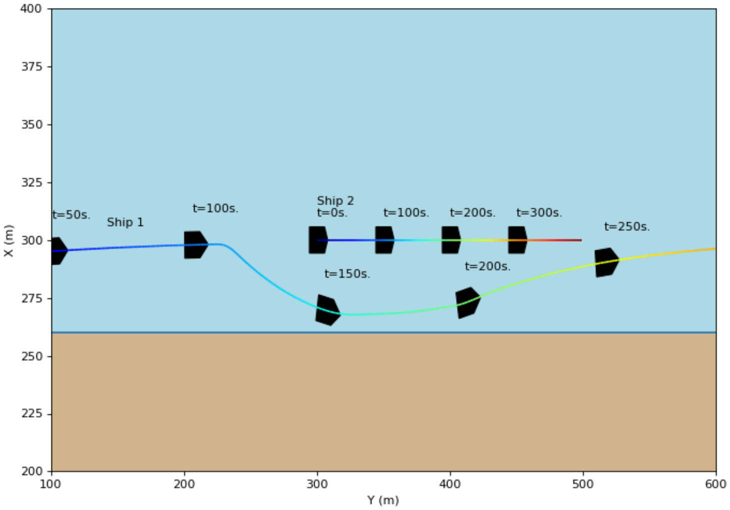

Figure 4.11: Simulation of the OS denoted Ship 1, overtaking the TS denoted Ship 2, in the presence of land.

stationary obstacle. When Ship 1 comes to close to the stationary obstacle it is repelled a bit, seen by the small alteration in its course. Ship 2 then passes Ship 1, giving Ship 1 a clear route, this ends up in a quite aggressive port side turn before Ship 1 converges back to its nominal path.

Give-way situation with shallow water.

In Figure 4.13, Ship 1 and Ship 2 holds the same nominal paths as the last scenario. In this scenario a stationary obstacle is placed as shallow water near where Ship 1 navigates when avoiding ship 2. Ship 1 is seen clearly avoiding the obstacle with a big starboard turn. Just afterwards Ship 1 makes this maneuver, Ship 2 passes Ship 1, giving Ship 1 clear route. Ship 1 can then start to converge towards its nominal path by taking a port side turn.

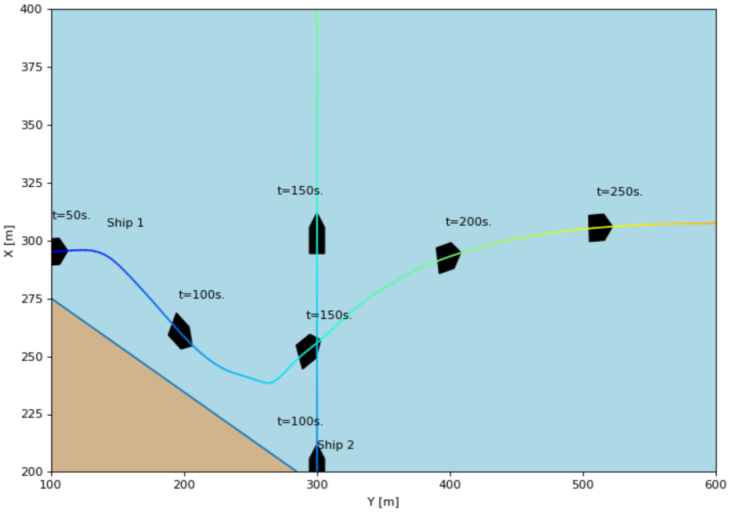

Figure 4.12: Simulation of the OS denoted, Ship 1 giving way to the TS denoted, Ship 2, in the presence of land.

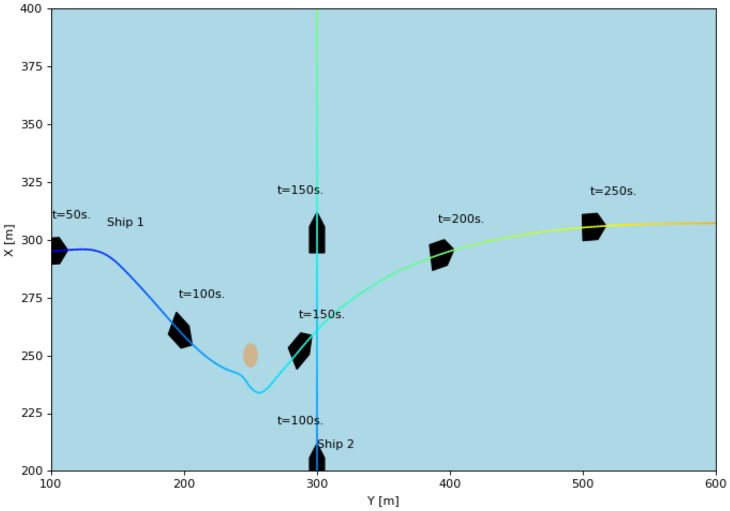

Figure 4.13: Simulation of the OS denoted Ship 1, giving way to the TS denoted Ship 2, in the presence of shallow water.

4.2.3 Two-ship encounters

In this section, three scenarios are presented. One OS and two TSs are included to create a situation where the OS must avoid colliding with both the TSs. For all the scenarios the OS has a nominal path that moves parallel to the Y axis at a constant velocity.

Give-way to overtaking situation

In Figure 4.14, a situation where the OS denoted Ship 1, first give-way to one TS denoted Ship 2, then overtake another TS denoted, Ship 3. Ship 2 has a path that moves parallel to the X axis at the same speed as Ship 1, while Ship 3 has a path that moves parallel to the Y axis at a lower speed than Ship 1. From the figure, it is clear to see that Ship 1 starts to perform a starboard turn to give way to Ship 2. When Ship 2 is out of harms way, Ship 1 corrects its heading towards the nominal path. It can however not converge to it, as it is influenced from the target ship domain of Ship 3, forcing Ship 1 to keep on the starboard side. When it then passes Ship 3, it can converge to its nominal path.

Overtake to overtake situation.

In Figure 4.15, the OS denoted Ship 1, must overtake two TSs; Ship 2 and Ship 3. Ship 2 has a path that is rotated 20 degrees counter clockwise from being parallel to the Y axis, and Ship 3 has a path that has only been rotated 10 degrees counter clockwise from being parallel to the Y axis. Ship 2 and Ship 3 keep the same speed, while Ship 1 is going faster than them. From the figure, it's clear Ship 1 turns to starboard to pass on the starboard side of Ship 2, when it has passed Ship 2 it holds it course for a moment, before Ship 1 then comes into contact with the target ship domain of Ship 3 and performs another starboard turn. Eventually it passes Ship 2 and converges back to the nominal path. In total Ship 1 maneuvers nicely past both the other ships. Since both ships are tucked nicely together it almost seems like it makes one big maneuver to pass them both.

Give-way to give-way situation.

In Figure 4.16, the OS must give-way to two TSs; Ship 2 and Ship 3. Ship 2 holds a path parallel with the X axis, while Ship 3's path is rotated 30 degrees counter clockwise in relative Ship 2's path. All the ships have the same speed. Ship 1 first make a starboard turn to pass behind Ship 2. Instead of converging back to the nominal path after it passes Ship 2, it keeps a somewhat constant course until it also passes behind Ship 3. In total Ship 1 navigates safely around both ships.

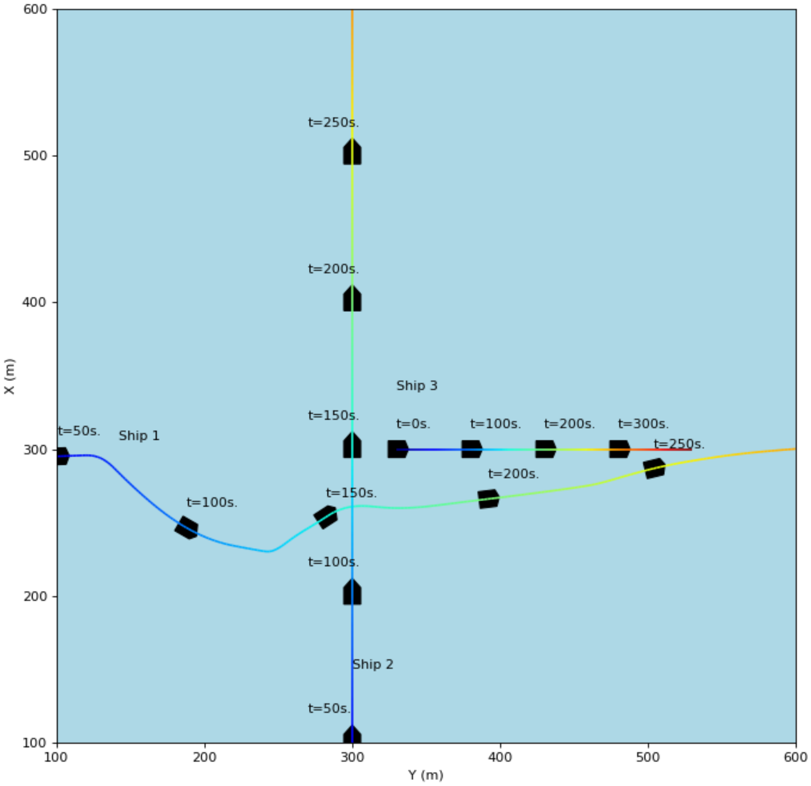

Figure 4.14: Simulation of the OS denoted Ship 1, first giving way to one TS denoted Ship 2 and then passing TS denoted Ship 3.

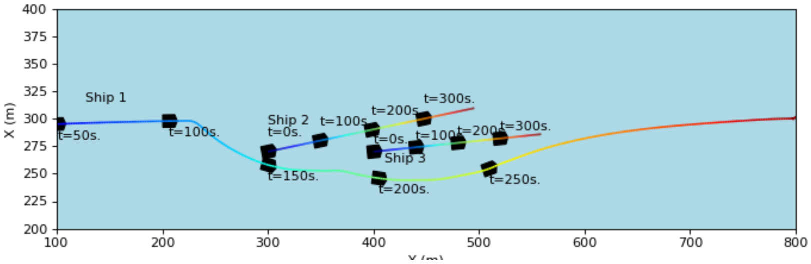

Figure 4.15: Simulation of the OS denoted Ship 1, first overtaking one TS denoted Ship 2, then overtaking another TS denoted Ship 3.

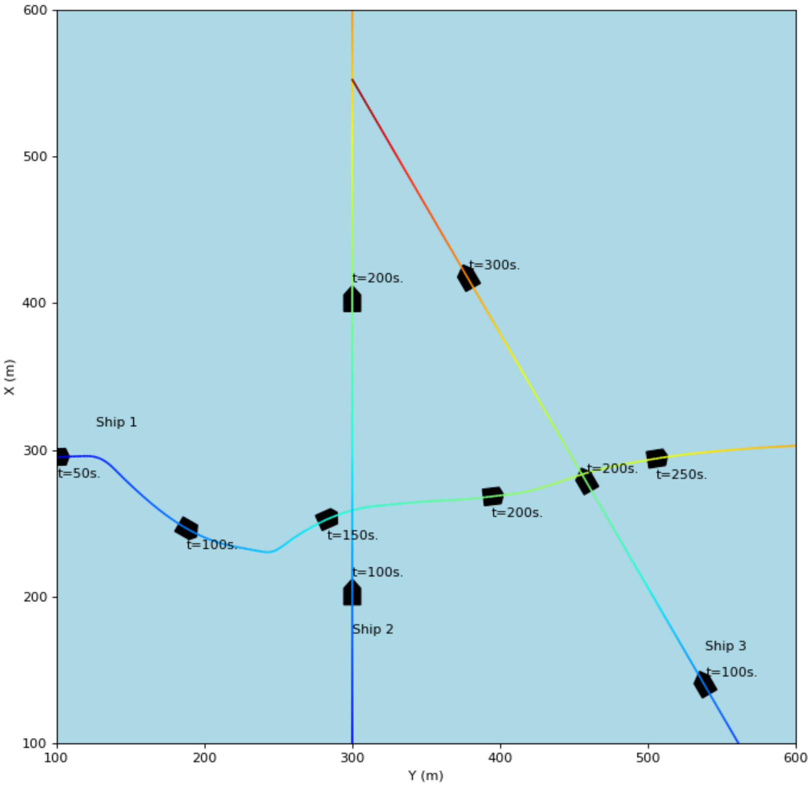

Figure 4.16: Simulation of the OS denoted Ship 1, first giving way to one TS denoted Ship 2, then giving way to another TS denoted Ship 3.

4.2.4 Navigating with multiple vessels

In this section, two scenarios are presented. In these scenarios three vessels are all navigating with the proposed COLAV method.

Three vessels navigating in open waters.

In Figure 4.17, three vessels are navigating in open waters. Ship 1 has a nominal path parallel to the Y axis, moving left to right. Ship 2's nominal path is also parallel to the Y axis, but moving right to left. Finally Ship 3 has a nominal path moving parallel with the X axis upwards. In this scenario Ship 1 and Ship 2 is in a head-on situation, while Ship 3 must give-way to ship 2. As seen in the figure, all the ships are navigating in accordance to

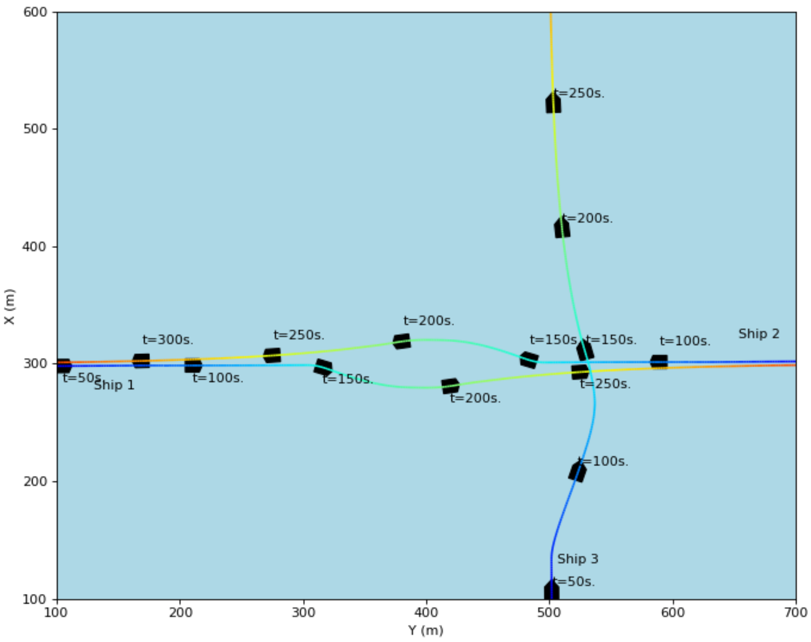

Figure 4.17: Three vessels navigating with the proposed COLAV method. Ship 1 and Ship 2 meeting head-on and Ship 1 giving way to Ship 3.

the COLREGs rules. They navigate smoothly, yet still have a sufficiently large correction in bearing signaling the evasive maneuver to the other ships.

Three vessels navigating in harbour.

In Figure 4.18, three vessels are navigating in a harbour like situation. Stationary obstacles are placed at points along the boarder of the harbor, such that the ships are repelled by it. Ship 1 has a nominal path parallel to the Y axis, stopping inside the harbour. Ship 2 is moving out of the harbour creating an attack angle between itself and Ship 1 of 165 degrees. Ship 3 is also starting in the harbour but has a nominal path that is parallel to the X axis. In this scenario, Ship 1 must give-way to Ship 3, and Ship 1 meets Ship 2 head-on. Ship 3 is the stand on vessel and can simply follow its nominal path. From the figure, it is clear that Ship 1 performs a starboard turn in order to pass behind Ship 3. Ship 1 and Ship 2 then both do a starboard turn making a head-on maneuver. Since there are some time between Ship 1 lets go of the target ship domain of Ship 3 and interacts with the target ship domain of Ship 2, it starts doing a port side turn towards it nominal path, when it clearly just could stay on the bearing around $t = 100s$ in order to pass on the starboard side of

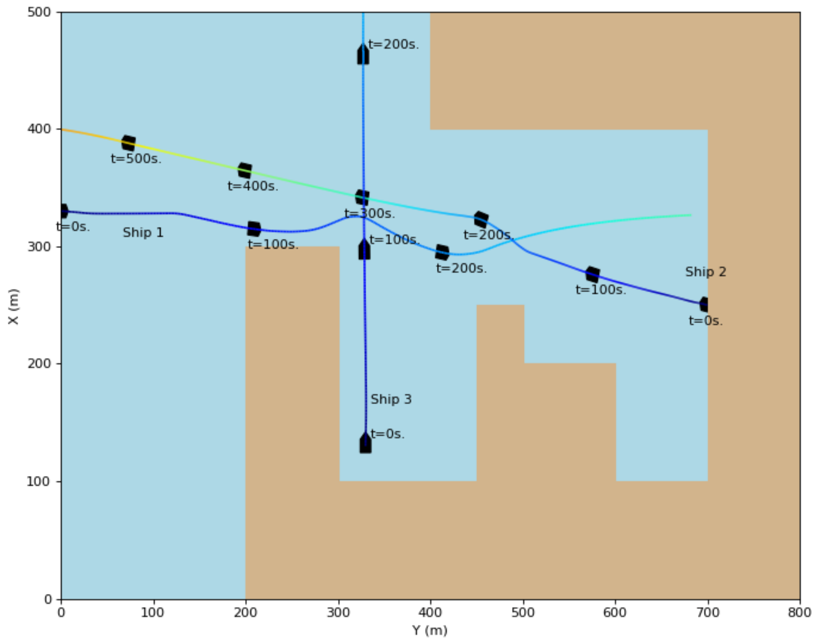

Figure 4.18: Three vessels navigating with the proposed COLAV method. Ship 1 meeting Ship 2 head-on and Ship 1 giving way to Ship 2.

Ship 2. In total the vessels maneuver in accordance to the COLREGs rules, but have some unnecessary maneuvering.

4.2.5 Performance boundaries

In this section, we attempt to highlight some performance boundaries of the method. That is, situations that test the performance of the proposed approach and results in undefined or undesired behaviour. This type of behaviour is produced by setting stationary obstacles in the way of where the OS would normally navigate to when avoiding a collision.

Overtaking in very tight waters.

In Figure 4.19, the OS denoted Ship 1 has a nominal path parallel to the Y axis. The TS denoted Ship 2 also has a path parallel to the Y axis, it however holds a lower speed than Ship 1. This creates a overtaking scenario, where Ship 1 must overtake Ship 2. Two stationary obstacles are placed on both sides of the vessels, producing a narrow channel only 40 meters wide. From the figure, Ship 1 can be seen making a starboard turn in order to pass on the starboard side of Ship 2. Ship 1 is then oscillating a bit. This happens as the vessel approach the stationary obstacle it is forced to make a port side turn avoiding the collision. This happens at the same time as the vessel is under the influence of the target ship domain. This situation produces somewhat of a war between the stationary obstacle and the target ship domain, where the stationary obstacle tries to push Ship 1 away from it and into a port side turn, and the target ship domain tries to push it towards a starboard turn. This leads to an unwanted behaviour of Ship 1. The oscillations themselves are quite bad with aggressive course changes, which is probably not very comfortable for passengers. Ship 1 is also scary close to Ship 2 when overtaking, which indicates that Ship 1 does not keep a safe distance to Ship 2 when performing the overtaking maneuver in this scenario.

Give-way with stationary obstacle blocking.

In Figure 4.20, the OS denoted Ship 1 has a nominal path parallel to the Y axis, and the TS denoted Ship 2 has a nominal path parallel to the X axis. This creates a give-way situation, where Ship 1 must give-way to Ship 2. A stationary obstacles is also placed in the bottom left corner of the figure. This obstacle is placed such that it mostly blocks Ship 1's opportunity to perform a proper starboard turn, and see how it then acts to still avoid the collision. In the figure, Ship 1 can be seen oscillating when it's under influence of both the target ship domain and the stationary obstacle, similar to the previous scenario.

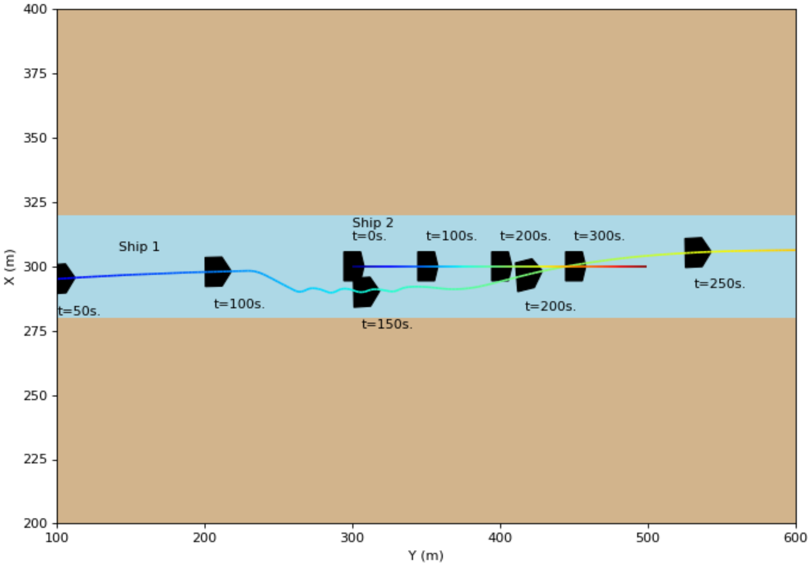

Figure 4.19: Simulation of the OS denoted Ship 1, overtaking the TS denoted Ship 2, in very tight waters.

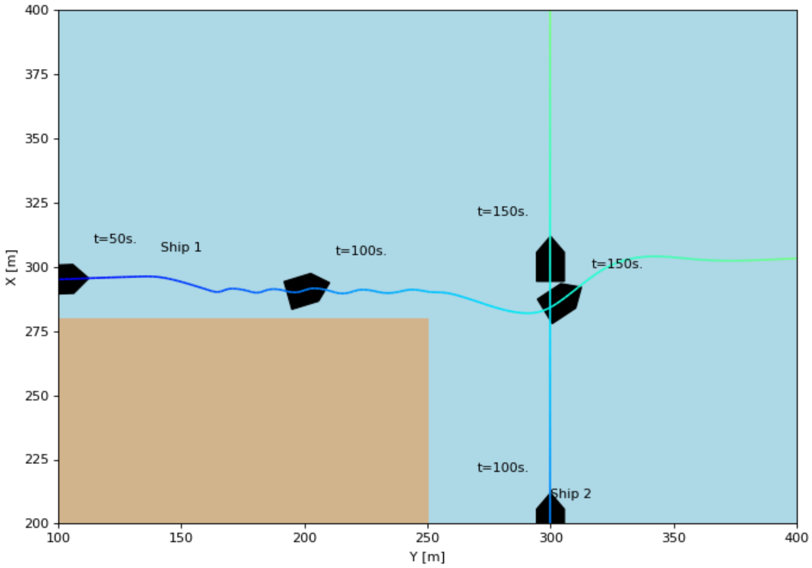

Figure 4.20: Simulation of the OS denoted Ship 1, giving way to the TS denoted Ship 2, with stationary obstacles blocking the intended path.

The oscillating movements work do in some ways slow down the vessel, as it uses longer time to navigate over a distance. When Ship 1 moves past the stationary obstacle is does a small starboard turn passing behind Ship 2. The distance between the vessels when Ship 1 navigates of the back of Ship 2 however seems to be quite small. And since this distance is so small, Ship 1 is inclined to fail to properly avoid the collision in this situation.

4.2.6 Minimum standard APF

In this section, a minimum standard APF is implemented to showcase the difference between the proposed COLREGs-aware target ship domain and a method without a COLREGs-aware target ship domain denoted as a minimum standard APF. The COLREGs unaware target ship domain is a target ship domain where the domain is created only by the position of the TS. The repulsive force is then created as a stationary obstacle placed at the position of the TS.

Overtake situation along land with minimum standard APF.

In this scenario, the same situation as in Figure 4.11, is tried with the minimum standard APF. The results from this is presented in Figure 4.21. There are some clear differences in the results between the two methods, the most obvious is that for minimum standard APF Ship 1 performs a port side turn to overtake Ship 2. Ship 1 does however not nearly have as smooth navigation when performing the overtaking maneuver as the proposed method has. When navigating with the minimum standard APF Ship 1 oscillates a lot. Ship 1 does however keep a good distance to Ship 2 during the entire maneuver.

Give-way situation along land with minimum standard APF.

In this scenario, the same situation as in Figure 4.12, is tried with the minimum standard APF. The results from this is presented in Figure 4.22. From the figure it is clear to see that Ship 1 is not navigating in accordance to the COLREGs rules. In this situation Ship 1 should give-way to Ship 2, which it certainly does not. The center of the repulsive field is stuck to the position of Ship 2 pointing away from it in every direction. As Ship 1 comes into contact with the repulsive field from Ship 2, it is forced to move upwards. And it is stuck in front of Ship 2 until it does a 360 degree maneuver and end up far enough away to not be influenced by the repulsive field any more. Then, Ship 1 converges nicely back to the nominal path.

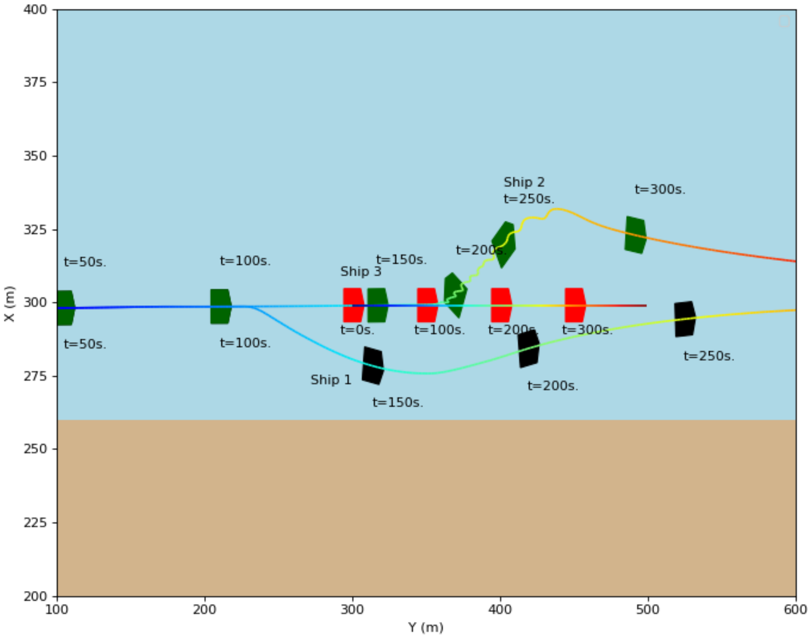

Figure 4.21: Comparison between the proposed method and a minimum standard APF in an overtake situation. The vessel running the proposed COLREGs-aware method is seen in black called Ship 1, while the vessel running the COLREGS unaware minimum standard APF is seen in dark green called Ship 2. Lastly the TS denoted Ship 3 is seen in red.

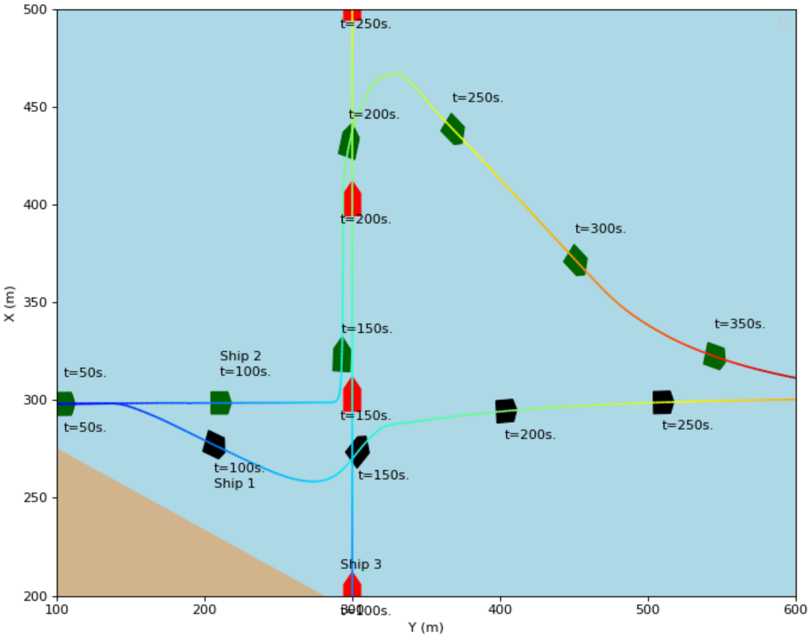

Figure 4.22: Comparison between the proposed method and a minimum standard APF i a give-way situation. The vessel running the proposed method is seen in black called Ship 1, while the vessel running the minimum standard APF is seen in dark green called Ship 2. Lastly the TS denoted Ship 3 is seen in red.

4.3 Discussion

From the simulation results presented in Section 4.2, it is clear that the method presented in this report is quite good. The performance of the method is verified for each of the chosen COLREGs rules through a series of batch plots, where the vessels approach with different attack angles. From the batch plots the method is proved to be quite robust under vessel to vessel (V2V) encounters. The method is further verified by introducing stationary obstacles acting as land or shallow water, where the OS navigates nicely around the obstacles. Further on, the OS must handle COLAV for multiple TSs, where both of the evasive maneuvers must come close together. The method seems to handle this nicely. The method is then executed on multiple vessels navigating in the same environment. The vessels here all show an expected behaviour, keeping away from stationary obstacles and performing COLREGs-compliant actions to avoid collisions.

In especially give-way scenarios the OS is seen having a quite aggressive heading change when it looses the contact with the target ship domain. This happens since the target ship domain has no influence on the total artificial potential force in the OS position. The goal position on the nominal trajectory is then the primary influence on the total potential artificial force, and further the desired states. This leads to this sudden alterations in heading, as the OS now wants to move towards the nominal trajectory.

The desire to move back to the nominal trajectory is also seen when the OS performs evasive maneuvers on multiple TSs. As the method is implemented independently on each of the TSs, the OS is seen trying to navigate back to the nominal trajectory in-between contact with the target ship domains. This is in some of the scenarios not beneficial, and the method would improve by handling multiple TSs better.

A slight concern is that the OS seems to pass quite close to the TSs at some of the scenarios. As the target ship domains distance is dependent on the distance between the vessels, it becomes much shorter when they are close together. The target ship domain is built up by a set number of points. The idea behind this is as the vessels come closer together the target ship domain is much more compact, and therefor has more of an influence on the total artificial potential force. The direction of the target ship domain however seem to be pointing too much towards the TS. And therefor causing the OS to pass close to the TS. There are multiple solutions to this problem. One is to place the target ship domain further away from the TS, and have the variable l to be more situational dependent. Having the variable α_{def} to be more situational dependent will also solve this problem. Lastly an interesting idea could be to have the target ship domain locked to the position the TS was k seconds ago. This would cause the OS to pass a clear distance from where the TS was instead of where it is.

From checking the limits of the method in Section 4.2.5, some of the method's largest weaknesses are presented. One of them is the clear oscillating behaviour the OS is presenting when the target ship domain pushes the ship one way, and the stationary obstacles push it in another. The situation in Figure 4.19, is constructed such that it is possible for the OS to stay parallel and close to the stationary obstacle, in order to perform the overtaking maneuver in a good way. One of the disadvantages with the target ship domain method in this type of scenario is shown through the oscillating behaviour. The method doesn't do any modifications to itself depending on the external factors. The distance l and the deflection angle α_{def} is set to a constant, when they should be situationally dependent. In a situation like Figure 4.19, the variables should be chosen such that when the OS is performing the overtake in a position where it's in a safe distance from the TS and the stationary obstacles, the target ship domain contributes to the X direction of the total artificial potential force by being the negative of the sum of the X component of the attractive field and the repulsive field from the stationary obstacle. This will cause the total artificial potential force to be 0 in the X direction, and the OS will navigate laterally with a constant distance between the TS and the stationary obstacles. From Figure 4.20 it's also clear that the OS could navigate better. As stated in Section 4.2.5, oscillations effectively slow down the vessel. A more suited way to navigate the vessel would then be to actually slow it down. This could be done by using the magnitude of the total artificial potential force to directly calculate the desired velocities, instead of finding them from the desired heading as in (3.16).

A general weakness for the implementation of the pipeline is that the stationary obstacles are not used to produce the most optimal navigation for the OS. In Figure 4.11, the OS can be seen taking a starboard turn in order to pass on the starboard side of the TS, when in fact it could be more beneficial to overtake on the port side, where there are no stationary obstacles. As the situational awareness module is implemented, the OS will always do a starboard turn in the situation in Figure 4.11, even if there is no room to pass on the starboard side of the TS. Especially for an overtake situation the situational awareness module should use the stationary obstacles to evaluate which side is possible to pass on.

Chapter 5

Conclusion and Future Work

In this Master's thesis, a COLREGs-aware collision avoidance (COLAV) method based on artificial potential fields (APFs) for autonomous surface vehicles (ASVs) has been presented. The method is based on COLREGs-specific target ship domains, constructed by the states of the OS and the TS. The APF method is then used to create reference states for the navigation of the OS. The proposed method has proven its performance through numerical simulations of simple V2V encounters, multi-ship encounters, and on static obstacles. The proposed method was also run on multiple vessels navigating in the same simulation environment. The proposed method proved through the numerical simulations to perform evasive maneuvers in compliance with COLREGs rules 13-15 and 17.

The proposed method was also compared to a minimum standard APF with a circular shaped target ship domain centered on the TS position. The proposed method proved to work much better, without the dramatic oscillations which the minimum standard APF produced.

The proposed method does however have room for improvement. When the OS is pressed in between the target ship domain and stationary obstacles, it showed signs of oscillating behaviour. The method also don't use the stationary obstacles to evaluate the situation. This could lead the OS into an undesirable path. There is also a chance for the OS to be caught in the target ship domain. This is however not a big issue as the direction of the repulsive forces from the target ship domain will eventually lead the OS away from it, and the target ship domain is removed from the environment when the OS has passed the TS.

Another weakness for the method is that it creates a target ship domain for each of the situations independently. In the time between performing the evasive maneuvers on a multi-ship encounter, the OS will start to navigate back towards it nominal path. It could however be more optimal to not go back to the nominal path between the encounters, and instead navigate parallel to the nominal path, in preparation for the next encounter.

The following should be investigated in future work:

- Include stationary obstacles in how the situation is categorized.
- Create a library that can be used as a lookup table to choose the correct parameters for the method.
- Use the forces from the APF directly to calculate the reference velocities.
- Expand the method to create multi target ship domains.
- Test the method in a real world scenario.

Bibliography

Cockcroft, A.N., Lameijer, J.N.F., 2012. Guide to the Collision Avoidance Rules. Butterworth-Heinemann.

Deng, F., Jin, L., Hou, X., Wang, L., Li, B., Yang, H., 2021. COLREGs: Compliant dynamic obstacle avoidance of USVs based on the dynamic navigation ship domain. Journal of Marine Science and Engineering 9, 837. doi:`10.3390/jmse9080837`.

Eriksen, B.O., Breivik, M., 2017. MPC-based mid-level collision avoidance for ASVs using nonlinear programming, in: IEEE Conference on Control Technology and Applications, Maui, Hawaii, USA.

Executive, T.M., . China launches its first autonomous container ship service. THE MARITIME EXECUTIVE URL: `https://www.maritime-executive.com/article/china-reports-first-autonomous-containership-entered-service`.

Fossen, T.I., 2000. A survey on nonlinear ship control: From theory to practice. IFAC Proceedings Volumes 33, 1–16. URL: `https://www.sciencedirect.com/science/article/pii/S1474667017370441`. 5th IFAC Conference on Manoeuvring and Control of Marine Craft (MCMC 2000), Aalborg, Denmark, 23-25 August 2000.

Fu-guang, D., Peng, J., Xin-qian, B., Hong-jian, W., 2005. AUV local path planning based on virtual potential field, in: IEEE International Conference Mechatronics and Automation, 2005, Niagara Falls, ON, Canada.

Huang, D., Liu, Z., Wang, X., 2020. Artificial potential field and ship maneuverability based collision avoidance path planning, in: 2020 Chinese Automation Congress (CAC), pp. 2490–2495. doi:`10.1109/CAC51589.2020.9327241`.

Khatib, O., 1985. Real-time obstacle avoidance for manipulators and mobile robots, in: 1985 IEEE International Conference on Robotics and Automation, St. Louis, USA. pp. 500–505.

Kirkerud, O.J.O., 2021. Collision avoidance for autonomous surface vehicles using artificial potential fields with colregs-aware target ship domains. Norwegian University of Science and Technology (NTNU), Trondheim, Norway .

Kufoalor, D.K., Brekke, E.F., Johansen, T.A., 2018. Proactive collision avoidance for asvs using a dynamic reciprocal velocity obstacles method, in: 2018 IEEE/RSJ International Conference on Intelligent Robots and Systems (IROS), pp. 2402–2409. doi:`10.1109/IROS.2018.8594382`.

Matoui, F., Boussaid, B., Mohamed Naceur, A., 2015. Local minimum solution for the potential field method in multiple robot motion planning task, in: 16th International Conference on Sciences and Techniques of Automatic Control and Computer Engineering, pp. 452–457.

NRK, . Trøndersk ferge til ol 2024. NRK URL: `https://www.nrk.no/trondelag/trondersk-ferge-til-ol-2024-1.15921884`.

Numpy, . About numpy. Numpy URL: `https://numpy.org/about/`.

Pedersen, A.A., 2019. Optimization based system identification for the milliampere ferry. Master's thesis, Norwegian University of Science and Technology (NTNU), Trondheim, Norway .

Press, T.A., . Driverless taxis are coming to the streets of san francisco. npr URL: `https://www.npr.org/2022/06/03/1102922330/driverless-self-driving-taxis-san-francisco-gm-cruise?t=1655150751233`.

Python, . About python. Python URL: `https://www.python.org/`.

Thyri, E.H., 2021. Classification of a vessel to vessel encounter, with respect to COLREGs. Norwegian University of Science and Technology (NTNU), Trondheim, Norway .

Appendix A

Appendix

A.1 Python implementation of Safe passage circle and closest point of approach method

```
def cpa_unsafe_passage(self, os_state, ts_state):
    #Python implementation of Safe passage circle and
    closest point of approach method

    #os_state, ts_state = np.array([x,y,psi,x_dot,y_dot, r])

    v_ab = np.array([os_state[3] - ts_state[3],
                    os_state[4]-ts_state[4]])

    p_ba = np.array([ts_state[0]- os_state[0],
                    ts_state[1] - os_state[1]])

    v_ab_abs = np.sqrt(v_ab[0]**2+v_ab[1]**2)


    if v_ab_abs > 0:
        t_ab = p_ba@v_ab.reshape(2,1)/v_ab_abs**2
        t_ab = t_ab[0]
    else:
        t_ab = 0

    d_ab = ((os_state[:2] + t_ab*os_state[3:5])-
            (ts_state[:2]+t_ab*ts_state[3:5]))
```

```
    d_ab = np.sqrt(d_ab[0]**2+d_ab[1]**2)

    return d_ab
```

A.2 Python implementation of the LOS guidance algorithm

```
def getGoal(self, t, eta):
    dist_low = math.sqrt((eta[0]-self.trajectory[i,-1])**2
                + (eta[1]-self.trajectory[i,-1])**2)

    for i in range(self.trajectory.shape[0]):
        dist = math.sqrt((eta[0]-self.trajectory[i,0])**2
                + (eta[1]-self.trajectory[i,1])**2)

        if(dist>self.dist_limit):
            heading = wrap_yaw(self.trajectory[i,2])

            theta = np.arctan2((eta[1]-self.trajectory[i,1]),
                               (eta[0]-self.trajectory[i,0]))

            if (wrap_yaw(theta-heading)>=-self.forward_min)
                and (wrap_yaw(theta-heading)<=self.forward_min)
                and  (dist<dist_low):

                dist_low = dist
                low_index = i

        elif(dist<self.dist_limit):
            low_index = self.sim_time-1

        else:
            low_index = self.sim_time-1

    return self.trajectory[low_index,:2]
```

A.3 Python implementation of a pid dp controller developed by the milliAmpere team.

```
def get_control_action(self):
    psi = self.eta[2]
    R = get_rotation_matrix(psi)
```

```
    eta_ref_ = self.eta_ref
    eta_ref_[2] = np.unwrap([self.eta[2], eta_ref_[2]])[1]

    eta_tilde = self.eta - eta_ref_
    eta_dot = R @ self.nu
    eta_dot_tilde = eta_dot - self.eta_dot_ref

    self.tau_i_ned = self.tau_i_ned - self.dt *
                    self.Gi @ eta_tilde

    self.tau_i_ned = np.clip(
                    self.tau_i_ned,
                    -self.tau_i_windup,
                    self.tau_i_windup)

    tau_p_ned = -self.Gp @ eta_tilde
    tau_i_ned = self.tau_i_ned
    tau_d_ned = -self.Gd @ eta_dot_tilde

    tau_pid_ned = tau_p_ned + tau_i_ned + tau_d_ned

    nu_ref = R.T @ self.eta_dot_ref
    nu_dot_ref = R.T @ self.eta_ddot_ref
    D = self.D_mtrx(nu_ref)

    tau_ff_acc = self.M @ nu_dot_ref
    tau_ff_vel = D @ nu_ref

    tau = \
        self.k_ff_acc * tau_ff_acc + \
        self.k_ff_vel * tau_ff_vel + \
        R.T @ tau_pid_ned

    return tau
```

A.4 Python implementation of a vessel model RK45 integrator.

```
def milliAmpere_vessel_dynamics_surge_decopuled(t,x):
# x is a vector of vessel states;
# x(1:3,1) is eta
# x(4:6,1) is nu
# x(7:9,1) is tau
```

```
    nu = x[3:6].reshape(3,1)
    [M,C,D] = comp_matrices_surge_decoupled(nu)
    thruster_tau = x[6:9]

    dxdt = np.array([0.0,0.0,0.0,0.0,0.0,0.0,0.0,0.0,0.0])

    # Calculate the nu dynamics
    dxdt[3:6] = np.matmul(np.linalg.inv(M),
                        np.add(thruster_tau.reshape(3,1),
                        - np.matmul(np.add(C,D),nu))).ravel()

    # eta_dynamics
    dxdt[0:3] = np.matmul(np.array([[np.cos(x[2]),-np.sin(x[2]), 0],
                                    [np.sin(x[2]), np.cos(x[2]), 0],
                                    [0, 0, 1]]),x[3:6].reshape(3,1))
                                    .ravel()
    return dxdt

def simulate_vessel_dynamics(eta, nu, tau):

    #Put all states in one vector
    x = np.array([eta,nu,tau]).ravel()

    #Use the RK45 from scipy to simulate the
    #vessel over a given time.
    #milliAmpere_vessel_dynamics_surge_decoupled
    #gives dxdt as a function of the states.

    solution = inte.RK45(milliAmpere_vessel_dynamics_surge_decopuled,
                        y0=x, t0 = 0, t_bound=1, max_step = 0.01)

    # collect data

    y_values = []
    for i in range(60):
        # get solution step state
        solution.step()
        y_values.append(solution.y[0])
        # break loop after modeling is finished
        if solution.status == 'finished':
            break

    eta = solution.y[0:3]
```

```
nu = solution.y[3:6]
eta[2] = solution.y[2]


return eta, nu
```

NTNU
Norwegian University of
Science and Technology